Table 1 Clinical findings and *HRAS* mutations in our CS patients

Patients	*NS71*	*NS123*	*NS125*	*NS132*	*NS137*	*NS139*	*NS156*	*NS157*	*NS167*	*NS181*	*NS198*	*NS217*
Gender	F	F	F	F	M	F	M	F	M	M	M	M
Age	9 months	11 years	17years	3 years	10 years	7 months	2 years 3 months	17 years	3 months	3 years	1 year 2 months	4 years 6 months
Paternal age at birth (years)	39	29	42	37	30	35	34	34	37	33	31	40
Maternal age at birth (years)	28	26	27	31	28	35	36	36	34	33	31	37
Growth and development												
Postnatal failure to thrive	+	+	+	+	+	+	+	+	+	+	+	+
Mental retardation	+	+	+	+	+	+	+	+	+	+	+	+
Craniofacial characteristics												
Relative macrocephaly	+	+	+	+	+	+	+	+	+	+	+	+
Coarse facial appearance	+	+	+	+	+	+	+	+	+	+	+	+
Muscloskeltal characteristics												
Short neck	+	+	+	+	+	+	+	+	–	+	–	+
Hyperextensive fingers	+	+	+	+	–	+	+	+	+	–	–	–
Tight Achilles tendon	–	+	+	+	+	–	+	–	–	–	–	+
Abnormal foot position	+	+	+	+	NA	+	NA	–	–	+	–	+
Skin characteristics												
Curly, sparse hair	+	+	+	+	+	+	+	+	+	+	Curly	+
Soft, loose skin	+	+	+	+	+	+	+	+	–	+	+	+
Deep palmer/ planter creases	+	+	+	+	+	+	+	+	+	+	+	+
Cardiac defect												
Hypertrophic cardiomyopathy	+	–	+	–	+	+	NA	+	–	+	–	–
Others	PS	–	–	–	–	–	PAC	Anomalous septum in the right atrium	VSD, arrhythmia	Atrial tachycardia	–	ASD, PSVT, PVC, CAR
Neoplasia												
Papillomata	–	–	+	–	–	–	NA	+	+	–	+	–
Other tumors		Bladder cancer							Heart neoplasia			
Others			GH deficiency		GSDIII	Chiari I, syringomyelia	Pyrolic stenosis	Congenial stridor, GH deficiency	Hypoplastic nails	Hypertention		Hydronephrosis, GER, laryngomalacia
HRAS mutation												
Nucleotide substitution	c.34G>A	c.35G>C	c.34G>A	c.34G>A	c.34G>A	c.34G>A	c.34G>A	c.34G>A	c.34G>A	c.34G>A	c.34G>A	c.34G>A
Amino acid substitution	p.G12S	p.G12A	p.G12S	p.G12S	p.G12S	p.G12S	p.G12S	p.G12S	p.G12S	p.G12S	p.G12S	p.G12S

Table 1 Continued

Patients	*NS223*	*NS231*	*NS239*	*NS248*	*NS254*	*NS263*	*NS299*	*NS318*	*NS324*	*Total*
Gender	F	F	M	M	F	M	F	F	F	
Age	6 months	5 months	18 years	5 years	2 months	1 month	3 years	1 month	1 year 6 months	
Paternal age at birth (years)	34	27	27	NA	37	35	34y	33	33	
Maternal age at birth (years)	36	27	26	30	34	36	35y	32	33	
Growth and development										
Postnatal failure to thrive	+	+	+	+	+	+	+	+	+	21/21
Mental retardation	+	+	+	+	NA	+	+	+	+	20/20
Craniofacial characteristics										
Relative macrocephaly	–	+	+	–	+	+	–	–	+	17/21
Coarse facial appearance	+	+	+	+	+	+	+	+	+	21/21
Muscloskeltal characteristics										
Short neck	–	+	NA	NA	+	+	+	–	–	14/19
Hyperextensive fingers	–	+	–	+	+	–	–	+	+	13/21
Tight Achilles tendon	+	NA	–	+	–	–	–	+	+	10/20
Abnormal foot position	–	–	NA	NA	NA	–	–	+	+	9/16
Skin characteristics										
Curly, sparse hair	+	Curly	Curly	+	+	+	Curly	+	Curly	21/21
Soft, loose skin	–	+	+	+	+	+	–	+	+	18/21
Deep palmer/planter creases	+	–	+	+	+	+	+	+	+	20/21
Cardiac defect										
Hypertrophic cardiomyopathy	+	–	+	+	+	+	+	+	+	14/20
Other	PAC	PVC	–	–	–	–	–	PAC	PAC	
Neoplasia										
Papillomata	+	–	+	–	–	–	–	–	–	6/20
Other tumors										
Others	Prabastatin administration	Laryngomalasia, hydrocephallus	GH deficiency, Arnold Chiari, scoliosis	Empty sella, GH deficiency, hypothyroidism, hypogonadism, syringomyelia	Hyperinsulinemia			Laryngomalasia seizure	Laryngomalasia	
HRAS mutation										
Nucleotide substitution	c.34G>T	c.35G>A	c.34G>A	c.34G>A	c.34G>A	c.35G>C	c.34G>A	c.35G>C	c.34G>A	
Amino acid substitution	p.G12C	p.G12D	p.G12S	p.G12S	p.G12S	p.G12A	p.G12S	p.G12A	p.G12S	

Abbreviations: –, absent; +, present; ASD, atrial septal defect; F, female; GER, gastroesophageal relfux; GH, growth hormone; GSDIII, glycogen storage disease III; M, male; NA, not available; PAC, premature atrial contraction; PS, pulmonic stenosis; PSVT, paroxysmal supraventricular tachycardia; PVC, premature ventricular contraction; VSD, ventricular septal defect.

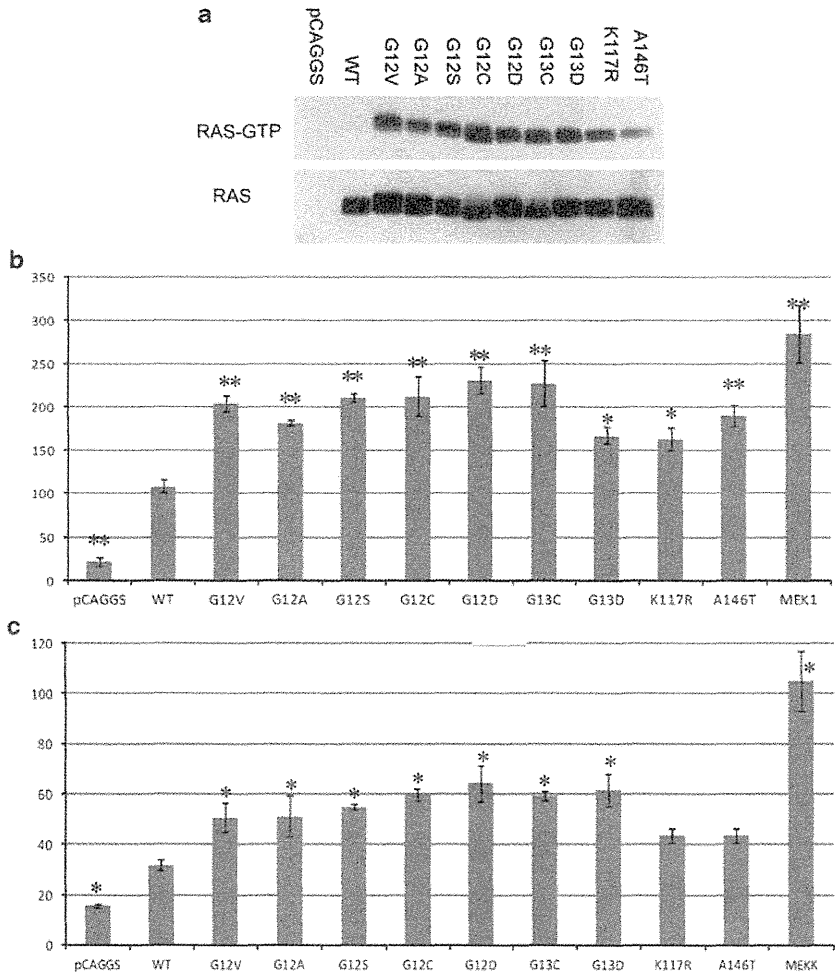

Figure 1 Functional characterization of HRAS mutants. (**a**) Ras-guanosine triphosphate (GTP) in NIH 3T3 cells transfected with wild-type or mutant HRAS constructs. HRAS protein levels were similar in NIH3T3 cells expressing each protein and were subsequently used as a loading control. (**b**, **c**) Stimulation of ELK (**b**) and c-Jun (**c**) transcription by *HRAS* mutants. The ELK-and c-Jun-GAL4 vectors and GAL4-luciferase trans-reporter vector were transiently co-transfected with various *HRAS* constructs into unstimulated NIH 3T3 cells. Relative luciferase activity (RLA) was normalized to the activity of a co-transfected control vector (phRLnull-luc) expressing *Renilla reniformis* luciferase. The results are expressed as the means and s.d. from triplicate samples. MEK1 and MEKK were used as positive controls. WT, wild type. $^{*}P<0.05$; $^{**}P<0.01$ compared with WT.

associated β-galactosidase staining confirmed that these cells showed cellular senescence.

Two downstream signaling pathways, p53 and Rb-p16, are activated during cellular senescence. To examine oncogene induced cellular senescence at the molecular level, we assessed senescence markers, including phosphorylated extracellular signal-regulated kinase, phosphorylated p53 and p16, in cells expressing HRAS mutant proteins (Figure 2b). As expected, phosphorylated p53 (Ser15) and p16 levels, as well as phospho-extracellular signal-regulated kinase levels, were significantly increased in the cells transfected with HRAS mutants relative to cells transfected with mock vector or wild-type HRAS. These results demonstrate that not only p.G12V, but also the other eight CS-related HRAS mutants, can cause OIS.

DISCUSSION

In this study, we identified four *HRAS* mutations in 21 patients with CS and evaluated their detailed clinical manifestations of the disease in these patients. Biochemical analyses, including a GTP binding assay and luciferase assays to detect ELK and c-Jun trans-activation, showed that there were no significant differences among the analyzed mutations in codon 12/13. The p.A146T mutant demonstrated the weakest Raf binding activity, and the p.K117R and p.A146T mutants had weaker effects on downstream c-Jun N-terminal kinase signaling than mutants in codon 12 or 13. Our results indicated that all HRAS mutants detected in CS patients were able to cause OIS.

Our study is the first to demonstrate that HRAS mutants other than p.G12V can induce senescence when they are overexpressed in human fibroblasts. The symptoms of CS seem to be caused by either hyperproliferation or hypoproliferation, coupled with growth factor resistance, which may be ascribable to DNA damage response or OIS. Postnatal cerebellar tonsillar herniation, Chiari 1 malformation,[42] deep palmar and plantar creases and papillomata may all be caused by hyperproliferation. In contrast, the poor weight gain, short stature and endocrine dysfunction observed in CS patients[43–45] might be caused by hypoproliferation. Adult brain and heart progenitor cells in a zebrafish CS model with a homozygous HRAS p.G12V mutation

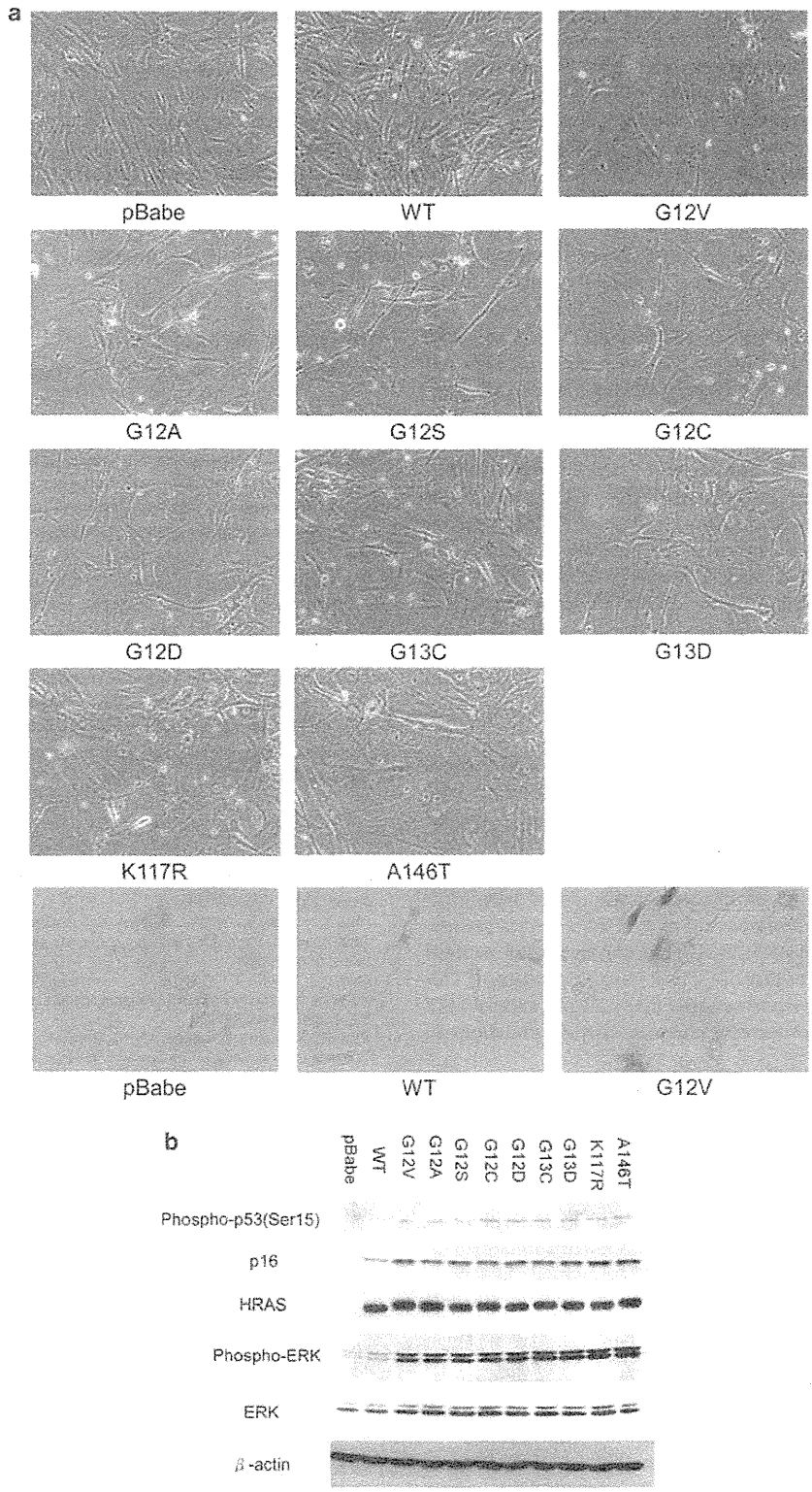

Figure 2 Effect of Costello syndrome (CS)-associated HRAS mutants on primary fibroblasts. (**a**) BJ cells transduced with retroviruses expressing wild-type or mutant HRAS. Images in the lowest tier show senescence-associated β-galactosidase staining. (**b**) Immunoblots of cellular lysates from BJ cells transduced with empty vector (pBabe) or with wild-type or mutant HRAS retroviruses.

exhibited cellular senescence, suggesting that the age-related worsening of the Costello phenotype[46] might occur, because the replicative capability of adult progenitor cells is exhausted. Osteoporosis has frequently been found in adult patients with CS,[47] suggesting that cellular senescence affects osteogenesis. However, further studies will be needed to determine whether OIS indeed contributes to the pathogenesis in patients with CS.

It has been suggested that clinical symptoms vary among patients with mutations in codon 12 or 13. In previous studies, a total of 19 CS patients have been reported to die from severe cardiomyopathy, cardiac arrhysmia, rhabdomyosarcoma, respiratory failure, multi-organ failure or sepsis. The number of fatal cases was 5/138 patients with p.G12S, 4/6 with p.G12C, 3/17 with p.G12A, 3/4 with p.G12D, 2/2 with p.G12V, 1/1 with p.G12E and 1/1 with p.E63K.[3,5–23] The mortality of patients with p.G12C or p.G12D was significantly higher than that of the patients with the more common p.G12S (P=0.026 by Fisher's exact test). Previous studies have shown that the p.G12V substitution has the highest transformative potential (p.G12V > p.G12A, p.G12S, p.G12C, p.G12D > p.G13D) and is the most frequently found mutation in human tumors.[48,49] However, our Ras activity assays and luciferase assays did not show any differences among *HRAS* codon 12/13 mutants. This may be due to the extremely high expression level of HRAS protein in our transient transfection study, which could make it difficult to detect subtle differences between mutants. Further studies will be necessary to clarify whether the high mortality in patients with p.G12C or p.G12D is due to functional differences in these mutants or due to bias because of our small sample size of patients.

Mutations at codons 117 and 146 are rare in CS and somatic cancers. Meanwhile, mutations at codons G12, G13 and Q61 have been shown to impair intrinsic and GTPase activating protein-mediated GTP hydrolysis, leading to elevated levels of cellular RAS-GTP. It has been reported that the nucleotide exchange rate of both p.K117R and p.A146V HRAS is increased, relative to wild type.[13,27,28] However, the transformational potential of p.A146V HRAS is partially activated,[27] whereas that of p.K117R-HRAS is not; its transformational activity is instead similar to that of GTPase impaired mutants.[28] Our results and those of other reports suggest that p.K117R and p.A146T have milder effects on downstream effectors than do mutations in codon 12/13.

The clinical manifestations of CS in patients with p.K117R or p.A146V mutations suggest that these alleles have distinct effects, compared with mutations in codon 12/13. Of two CS patients with a p.K117R mutation, one patient had an atypical phenotype such as microretrognatism and slightly less-pronounced plantar and palmar creases.[7] The other patient had mild craniofacial manifestations of CS.[13] One patient with the p.A146V mutation showed a mildly coarse face and did not have deep palmar creases.[6] These atypical phenotypes might be attributed to the mild effects of p.K117R or p.A146V compared with codon 12/13 mutants.

Inhibitors of the RAS/MAPK pathway could provide benefits for patients with RAS/MAPK syndromes. Statins are 3-hydroxy-3-methyl-glutaryl-CoA reductase inhibitors that result in decreased isoprenylation of RAS[50] and are now widely used for the treatment of hyperlipidemia. Statins have been used to modify the clinical manifestation of neurofibromatosis type I, which is caused by a genetic defect in a negative regulator of the RAS/MAPK pathway. Studies using mouse models of NF1 (Nf1 mice) have shown that treatment with a statin reverses the cognitive deficits of these mice.[51] A randomized control trial for neurofibromatosis type I treatment with simvastatin had a negative outcome.[52] Furthermore, statins have displayed antitumor activity in experimental tumor models, though clinical antitumor effects of statins have not been established.[53] Well-designed clinical studies will be needed to determine the effects of statins or other RAS inhibitors on manifestations of CS.

In conclusion, we identified *HRAS* mutations in 21 patients and examined the clinical manifestations of mutation-positive patients. Functional analysis revealed that CS-causing mutant HRAS proteins caused OIS in human fibroblasts. These findings may help enable more accurate prognoses for patients with *HRAS* mutations and contribute to our understanding of the mechanism underlying CS pathogenesis.

CONFLICT OF INTEREST

The authors declare no conflict of interest.

ACKNOWLEDGEMENTS

We thank the patients who participated in this study and their families and doctors, including Naoki Watanabe and Tomohiro Iwasaki, who referred the cases. We are grateful to Dr Garry Nolan of Stanford University for supplying Phoenix-Eco and Ampho cells, to Dr William C Hahn for supplying the pBabe-zeo-ecotropic receptor vector, and to Dr Jun-ichi Miyazaki of Osaka University for supplying the pCAGGS expression vector. We are also grateful to Drs Noriko Ishida and Keiko Nakayama for their technical assistance with the infection of retroviral vectors. We thank Kumi Kato and Hasumi Haba for their technical assistance. This work was supported by Grants-in-Aids for young scientists (A and S) from the Ministry of Education, Culture, Sports, Science and Technology of Japan (nos. 19689022, 21689029 and 19679005) to TN and YA, the Science and Technology Foundation of Japan Grant-in-Aid for Scientific Research to TN, and the Ministry of Health, Labour and Welfare to YM and YA.

1 Hennekam, R. C. Costello syndrome: an overview. *Am. J. Med. Genet. C. Semin. Med. Genet.* **117C,** 42–48 (2003).
2 Aoki, Y., Niihori, T., Narumi, Y., Kure, S. & Matsubara, Y. The RAS/MAPK syndromes: novel roles of the RAS pathway in human genetic disorders. *Hum. Mutat.* **29,** 992–1006 (2008).
3 Aoki, Y., Niihori, T., Kawame, H., Kurosawa, K., Ohashi, H., Tanakam, Y. *et al.* Germline mutations in HRAS proto-oncogene cause Costello syndrome. *Nat. Genet.* **37,** 1038–1040 (2005).
4 Kerr, B., Allanson, J., Delrue, M. A., Gripp, K. W., Lacombe, D., Lin, A. E. *et al.* The diagnosis of Costello syndrome: nomenclature in Ras/MAPK pathway disorders. *Am. J. Med. Genet. A* **146A,** 1218–1220 (2008).
5 Estep, A. L., Tidyman, W. E., Teitell, M. A., Cotter, P. D. & Rauen, K. A. HRAS mutations in Costello syndrome: detection of constitutional activating mutations in codon 12 and 13 and loss of wild-type allele in malignancy. *Am. J. Med. Genet. A.* **140,** 8–16 (2006).
6 Gripp, K. W., Lin, A. E., Stabley, D. L., Nicholson, L., Scott, C. I. Jr, Doyle, D. *et al.* HRAS mutation analysis in Costello syndrome: genotype and phenotype correlation. *Am. J. Med. Genet. A.* **140,** 1–7 (2006).
7 Kerr, B., Delrue, M. A., Sigaudy, S., Perveen, R., Marche, M., Burgelin, I. *et al.* Genotype-phenotype correlation in Costello syndrome: HRAS mutation analysis in 43 cases. *J. Med. Genet.* **43,** 401–405 (2006).
8 van Steensel, M. A., Vreeburg, M., Peels, C., van Ravenswaaij-Arts, C. M., Bijlsma, E., Schrander-Stumpel, C. T. *et al.* Recurring HRAS mutation G12S in Dutch patients with Costello syndrome. *Exp. Dermatol.* **15,** 731–734 (2006).
9 Gripp, K. W., Lin, A. E., Nicholson, L., Allen, W., Cramer, A., Jones, K. L. *et al.* Further delineation of the phenotype resulting from BRAF or MEK1 germline mutations helps differentiate cardio-facio-cutaneous syndrome from Costello syndrome. *Am. J. Med. Genet. A.* **143A,** 1472–1480 (2007).
10 Orstavik, K. H., Tangeraas, T., Molven, A. & Prescott, T. E. Distal phalangeal creases—a distinctive dysmorphic feature in disorders of the RAS signalling pathway? *Eur. J. Med. Genet.* **50,** 155–158 (2007).
11 Sovik, O., Schubbert, S., Houge, G., Steine, S. J., Norgard, G., Engelsen, B. *et al. De novo* HRAS and KRAS mutations in two siblings with short stature and neuro-cardio-facio-cutaneous features. *J. Med. Genet.* **44,** e84 (2007).
12 Zampino, G., Pantaleoni, F., Carta, C., Cobellis, G., Vasta, I., Neri, C. *et al.* Diversity parental germline origin, and phenotypic spectrum of *de novo* HRAS missense changes in Costello syndrome. *Hum. Mutat.* **28,** 265–272 (2007).
13 Denayer, E., Parret, A., Chmara, M., Schubbert, S., Vogels, A., Devriendt, K. *et al.* Mutation analysis in Costello syndrome: functional and structural characterization of the HRAS pLys117Arg mutation. *Hum. Mutat.* **29,** 232–239 (2008).

14 Gripp, K. W., Innes, A. M., Axelrad, M. E., Gillan, T. L., Parboosingh, J. S., Davies, C. *et al.* Costello syndrome associated with novel germline HRAS mutations: an attenuated phenotype? *Am. J. Med. Genet. A.* **146A,** 683–690 (2008).
15 Hou, J. W. Rapidly progressive scoliosis after successful treatment for osteopenia in Costello syndrome. *Am. J. Med. Genet. A.* **146,** 393–396 (2008).
16 Limongelli, G., Pacileo, G., Digilio, M. C., Calabro, P., Di Salvo, G., Rea, A. *et al.* Severe, obstructive biventricular hypertrophy in a patient with Costello syndrome: clinical impact and management. *Int. J. Cardiol.* **130,** e108–e110 (2008).
17 Schulz, A.L., Albrecht, B., Arici, C., van der Burgt, I., Buske, A., Gillessen-Kaesbach, G. *et al.* Mutation and phenotypic spectrum in patients with cardio-facio-cutaneous and Costello syndrome. *Clin. Genet.* **73,** 62–70 (2008).
18 Gremer, L., De Luca, A., Merbitz-Zahradnik, T., Dallapiccola, B., Morlot, S., Tartaglia, M. *et al.* Duplication of Glu37 in the switch I region of HRAS impairs effector/GAP binding and underlies Costello syndrome by promoting enhanced growth factor-dependent MAPK and AKT activation. *Hum. Mol. Genet.* **19,** 790–802 (2010).
19 Kuniba, H., Pooh, R.K., Sasaki, K., Shimokawa, O., Harada, N., Kondoh, T. *et al.* Prenatal diagnosis of Costello syndrome using 3D ultrasonography amniocentesis confirmation of the rare HRAS mutation G12D. *Am. J. Med. Genet. A.* **149A,** 785–787 (2009).
20 Lin, A. E., O'Brien, B., Demmer, L. A., Almeda, K. K., Blanco, C. L., Glasow, P. F. *et al.* Prenatal features of Costello syndrome: ultrasonographic findings and atrial tachycardia. *Prenat. Diagn.* **29,** 682–690 (2009).
21 Piccione, M., Piro, E., Pomponi, M. G., Matina, F., Pietrobono, R., Candela, E. *et al.* A premature infant with Costello syndrome due to a rare G13C HRAS mutation. *Am. J. Med. Genet. A.* **149A,** 487–489 (2009).
22 Sol-Church, K., Stabley, D. L., Demmer, L. A., Agbulos, A., Lin, A. E., Smoot, L. *et al.* Male-to-male transmission of Costello syndrome: G12S HRAS germline mutation inherited from a father with somatic mosaicism. *Am. J. Med. Genet. A.* **149A,** 315–321 (2009).
23 Zhang, H., Ye, J. & Gu, X. Recurring G12S mutation of HRAS in a Chinese child with Costello syndrome with high alkaline phosphatase level. *Biochem. Genet.* **47,** 868–871 (2009).
24 van der Burgt, I., Kupsky, W., Stassou, S., Nadroo, A., Barroso, C., Diem, A. *et al.* Myopathy caused by HRAS germline mutations: implications for disturbed myogenic differentiation in the presence of constitutive HRas activation. *J. Med. Genet.* **44,** 459–462 (2007).
25 McGrath, J. P., Capon, D. J., Goeddel, D. V. & Levinson, A. D. Comparative biochemical properties of normal and activated human ras p21 protein. *Nature.* **310,** 644–649 (1984).
26 Al-Mulla, F., Milner-White, E. J., Going, J. J. & Birnie, G. D. Structural differences between valine-12 and aspartate-12 Ras proteins may modify carcinoma aggression. *J. Pathol.* **187,** 433–438 (1999).
27 Feig, L. A. & Cooper, G. M. Relationship among guanine nucleotide exchange, GTP hydrolysis, and transforming potential of mutated ras proteins. *Mol. Cell. Biol.* **8,** 2472–2478 (1988).
28 Der, C. J., Weissman, B. & Macdonald, M. J. Altered guanine-nucleotide binding and H-Ras transforming and differentiating activities. *Oncogene.* **3,** 105–112 (1988).
29 Sikora, E., Arendt, T., Bennett, M. & Narita, M. Impact of cellular senescence signature on ageing research. *Ageing Res. Rev.* **10,** 146–152 (2010).
30 Serrano, M., Lin, A. W., McCurrach, M. E., Beach, D. & Lowe, S. W. Oncogenic ras provokes premature cell senescence associated with accumulation of p53 and p16INK4a. *Cell* **88,** 593–602 (1997).
31 Narita, M., Nunez, S., Heard, E., Narita, M., Lin, A. W., Hearn, S. A. *et al.* Rb-mediated heterochromatin formation and silencing of E2F target genes during cellular senescence. *Cell* **113,** 703–716 (2003).
32 Di Micco, R., Fumagalli, M., Cicalese, A., Piccinin, S., Gasparini, P., Luise, C. *et al.* Oncogene-induced senescence is a DNA damage response triggered by DNA hyper-replication. *Nature* **444,** 638–642 (2006).
33 Bartkova, J., Rezaei, N., Liontos, M., Karakaidos, P., Kletsas, D., Issaeva, N. *et al.* Oncogene-induced senescence is part of the tumorigenesis barrier imposed by DNA damage checkpoints. *Nature* **444,** 633–637 (2006).
34 Narita, M. & Lowe, S. W. Senescence comes of age. *Nat. Med.* **11,** 920–922 (2005).
35 Campisi, J. Suppressing cancer: the importance of being senescent. *Science* **309,** 886–887 (2005).
36 Kawame, H., Matsui, M., Kurosawa, K., Matsuo, M., Masuno, M., Ohashi, H. *et al.* Further delineation of the behavioral and neurologic features in Costello syndrome. *Am. J. Med. Genet. A.* **118A,** 8–14 (2003).
37 Kalfa, D., Fraisse, A. & Kreitmann, B. Medical and surgical perspectives of cardiac hypertrophy in Costello syndrome. *Cardiol. Young* **19,** 644–647 (2009).
38 Digilio, M. C., Sarkozy, A., Capolino, R., Chiarini Testa, M. B., Esposito, G., de Zorzi, A. *et al.* Costello syndrome: clinical diagnosis in the first year of life. *Eur. J. Pediatr.* **167,** 621–628 (2008).
39 Schuhmacher, A. J., Guerra, C., Sauzeau, V., Canamero, M., Bustelo, X. R. & Barbacid, M. A mouse model for Costello syndrome reveals an Ang II-mediated hypertensive condition. *J. Clin. Invest.* **118,** 2169–2179 (2008).
40 Kaji, M., Kurokawa, K., Hasegawa, T., Oguro, K., Saito, A., Fukuda, T. *et al.* A case of Costello syndrome and glycogen storage disease type III. *J. Med. Genet.* **39,** E8 (2002).
41 Omori, I., Shimizu, M. & Watanabe, T. An infant with Costello syndrome and a rare HRAS mutation (G12C). *J. Jpn. Pediatr. Soc.* **114,** 1592–1597 (2010).
42 Gripp, K. W., Hopkins, E., Doyle, D. & Dobyns, W.B. High incidence of progressive postnatal cerebellar enlargement in Costello syndrome: brain overgrowth associated with HRAS mutations as the likely cause of structural brain and spinal cord abnormalities. *Am. J. Med. Genet. A.* **152A,** 1161–1168 (2010).
43 Gregersen, N. & Viljoen, D. Costello syndrome with growth hormone deficiency and hypoglycemia: a new report and review of the endocrine associations. *Am. J. Med. Genet. A.* **129A,** 171–175 (2004).
44 Stein, R. I., Legault, L., Daneman, D., Weksberg, R. & Hamilton, J. Growth hormone deficiency in Costello syndrome. *Am. J. Med. Genet. A.* **129A,** 166–170 (2004).
45 Alexander, S., Ramadan, D., Alkhayyat, H., Al-Sharkawi, I., Backer, K. C., El-Sabban, F. *et al.* Costello syndrome and hyperinsulinemic hypoglycemia. *Am. J. Med. Genet. A.* **139,** 227–230 (2005).
46 Santoriello, C., Deflorian, G., Pezzimenti, F., Kawakami, K., Lanfrancone, L., d'Adda di Fagagna, F. *et al.* Expression of H-RASV12 in a zebrafish model of Costello syndrome causes cellular senescence in adult proliferating cells. *Dis. Model. Mech.* **2,** 56–67 (2009).
47 White, S. M., Graham, J. M. Jr, Kerr, B., Gripp, K., Weksberg, R., Cytrynbaum, C. *et al.* The adult phenotype in Costello syndrome. *Am. J. Med. Genet. A.* **136,** 128–135 (2005).
48 Seeburg, P. H., Colby, W. W., Capon, D. J., Goeddel, D. V. & Levinson, A. D. Biological properties of human c-Ha-ras1 genes mutated at codon 12. *Nature* **312,** 71–75 (1984).
49 Fasano, O., Aldrich, T., Tamanoi, F., Taparowsky, E., Furth, M. & Wigler, M. Analysis of the transforming potential of the human H-ras gene by random mutagenesis. *Proc. Natl Acad. Sci. USA* **81,** 4008–4012 (1984).
50 Jakobisiak, M. & Golab, J. Statins can modulate effectiveness of antitumor therapeutic modalities. *Med. Res. Rev.* **30,** 102–135 (2010).
51 Li, W., Cui, Y., Kushner, S. A., Brown, R. A., Jentsch, J. D., Frankland, P. W. *et al.* The HMG-CoA reductase inhibitor lovastatin reverses the learning and attention deficits in a mouse model of neurofibromatosis type 1. *Curr. Biol.* **15,** 1961–1967 (2005).
52 Krab, L. C., de Goede-Bolder, A., Aarsen, F. K., Pluijm, S. M., Bouman, M. J., van der Geest, J. N. *et al.* Effect of simvastatin on cognitive functioning in children with neurofibromatosis type 1: a randomized controlled trial. *JAMA* **300,** 287–294 (2008).
53 Dale, K. M., Coleman, C. I., Henyan, N. N., Kluger, J. & Whitem, C. M. Statins and cancer risk: a meta-analysis. *JAMA* **295,** 74–80 (2006).

ELSEVIER

Brain & Development 33 (2011) 576–579

BRAIN & DEVELOPMENT
Official Journal of the Japanese Society of Child Neurology

www.elsevier.com/locate/braindev

Original article

A familial case of LEOPARD syndrome associated with a high-functioning autism spectrum disorder

Yoriko Watanabe [a,1,*], Shoji Yano [b], Tetsuya Niihori [c], Yoko Aoki [c], Yoichi Matsubara [c], Makoto Yoshino [a], Toyojiro Matsuishi [a,1]

[a] *Department of Pediatrics and Child Health, Kurume University School of Medicine, 67 Asahi-machi, Kurume, Japan*
[b] *Genetics Division, Department of Pediatrics, LAC+USC Medical Center, Keck School of Medicine, University of Southern California, Los Angeles, CA, USA*
[c] *Department of Medical Genetics, Tohoku University School of Medicine, Sendai, Japan*

Received 6 July 2010; received in revised form 3 October 2010; accepted 6 October 2010

Abstract

A connection between LEOPARD syndrome (a rare autosomal dominant disorder) and autism spectrum disorders (ASDs) may exist. Of four related individuals (father and three sons) with LEOPARD syndrome, all patients exhibited clinical symptoms consistent with ASDs. Findings included aggressive behavior and impairment of social interaction, communication, and range of interests. The coexistence of LEOPARD syndrome and ASDs in the related individuals may be an incidental familial event or indicative that ASDs is associated with LEOPARD syndrome. There have been no other independent reports of the association of LEOPARD syndrome and ASDs. Molecular and biochemical mechanisms that may suggest a connection between LEOPARD syndrome and ASDs are discussed.

Keywords: LEOPARD syndrome, Noonan syndrome; Autism spectrum disorders (ASDs); RAS/MAPK signal transduction pathway

1. Introduction

LEOPARD syndrome (OMIM#151100) is a rare autosomal dominant disorder characterized by Lentigines, Electrocardiogram abnormalities, Ocular hypertelorism, Pulmonic valvular stenosis, Abnormalities of genitalia, Retardation of growth, and Deafness. This syndrome is caused by germline missense mutations in the *PTPN11* gene that encodes Src homology 2 domain-containing tyrosine phosphatase 2 (Shp2): non-receptor protein-tyrosine phosphatase comprising two N-terminal SH2 domains, a catalytic domain, and a C terminus with tyrosylphosphorylation sites and a proline-rich stretch. The mutations induce catalytically impaired Shp2 by a "dominant negative effect" [1–2].

In the more common Noonan syndrome, approximately 50% of patients have *PTPN11* mutations scattered over the entire Shp2, including the catalytic domain. The mutations resulting in the Noonan phenotype are the "gain-of-function" mutations, and they exhibit substantially increased catalytic ability. Although LEOPARD syndrome and Noonan syndrome are caused by *PTPN11* mutations resulting in opposite effects, they share many common clinical features, including physical dysmorphic findings and intellectual disability [1].

The term "autism spectrum disorders (ASDs)" was first used by Lorna Wing [3] and then widely used as a category comprised of autistic disorder, Asperger's

* Corresponding author. Tel.: +81 942 35 3311x3656; fax: +81 942 38 1792.
E-mail address: york@med.kurume-u.ac.jp (Y. Watanabe).
[1] The author contributed equally to this work.

0387-7604/$ - see front matter © 2010 The Japanese Society of Child Neurology. Published by Elsevier B.V. All rights reserved.
doi:10.1016/j.braindev.2010.10.006

disorder, and other related conditions [4]. These conditions are very common neurobehavioral disorders that are characterized by impairments in three behavioral domains, including social interaction, language/communication/imaginative play, and a range of interests and activities [3–5].

At least ten genes have been reported to be associated with ASDs [6]. Except for Rett syndrome, the other pervasive developmental disorder (PDD) subtypes including autistic disorder, Asperger's disorder, disintegrative disorder, and PDD Not Otherwise Specified (PDDNOS) are not tightly linked to any particular gene mutations. Several common genetic syndromes are known to be associated with ASDs. Autism is frequent in patients with tuberous sclerosis (TSC) [7], with neurofibromatosis type 1 [8,9] and with Fragile X syndrome [10]. Studies of psychological profiles of adults with Noonan syndrome did not suggest a specific behavioral phenotype, but difficulties with social competence and emotional perceptions were noted [11]. A case of Noonan syndrome who was also diagnosed with autism was reported [12]. The present study of neuropsychiatric evaluation in a familial case of LEOPARD syndrome indicates all patients satisfied the criteria of ASDs. An association of LEOPARD syndrome and ASDs has not been reported previously. The familial case presented in this report may suggest such an association.

2. Patients and methods

After obtaining written informed consent, fifteen coding exons in *PTPN11* were sequenced in each patient following the methods described somewhere else [13].

Diagnostic and Statistical Manual of Mental Disorders, Fourth Edition (DSM-IV-TR) [5] and The high-functioning Autism Spectrum Screening Questionnaire (ASSQ) [14] were used in neuropsychiatric evaluation of the subjects.

Patient 1 is a 20-year-old male who was born as the second child to a non-consanguineous Japanese couple. His early developmental milestones were reportedly unremarkable. He was clinically diagnosed with LEOPARD syndrome at age 7 years based on findings that included lentigines, multiple café-au-lait spots, electrocardiogram (ECG) abnormalities, ventricular septal defect, ocular hypertelorism, short stature, and unilateral renal hypoplasia. *PTPN11* mutation analysis revealed a heterozygous mutation of 1403C > T (T468 M). The patient was diagnosed as having Asperger's disorder based on ASSQ and DSM-IV-TR, at age 12 years. His intelligence quotient (IQ) by the Wechsler Intelligence Scale for Children-third edition (WISC-III) was 85 (verbal: 77, performance 98). His ASSQ score by mother's rating was 41. He met the DSM-IV-TR diagnostic criteria of Asperger's disorder with all subcategories in the category of Qualitative impairment in social interaction (Category 1), three subcategories (1,2, and 4) in the category of Restricted repetitive and stereotyped patterns of behavior, interests and activities (Category 2), and the rest of the four categories (Table 1).

Patient 2 is a 15-year-old younger brother of Patient 1. His early infantile developmental milestones were unremarkable. He was diagnosed with growth retardation at age 2½ years. At age 12 years his clinical findings of a few café-au-lait spots, ocular hypertelorism, and undescended testes led us to obtain *PTPN11* mutation analysis, which showed the same heterozygous mutation of 1403C > T. At age 9 years, a diagnosis of Asperger's disorder was made based on ASSQ and DSM-IV-TR. His full-scale IQ by WISC-III at age 9 years was 99 (verbal 104, performance 92). His ASSQ score by parental rating was 32 at age 15 years. He also met the Asperger's disorder diagnostic criteria with all subcategories of Category 1, three of Category 2 (1, 2, and 4), and the rest of the categories (Table 1).

Patient 3 is the 22-year-old eldest brother of Patients 1 and 2. His developmental milestones were normal, although his ritualistic behavior and difficulties in relating to peers were noted in his childhood. He had a surgical repair of bilateral undescended testes and inguinal hernia. He was diagnosed with Wolff-Parkinson-White syndrome at age nine years. He has ocular hypertelorism and short stature. The same *PTPN11* heterozygous mutation found in the two younger siblings was identified in this patient. He attends college, and was diagnosed as having PDDNOS, because he also had impaired development of reciprocal social interaction associated with communication skills, repetitive routine, and ritualistic behavior. His ASSQ score was 7 at age 22 years (Table 1).

Patient 4 is a 55-year-old male who is the father of the siblings. He has prominent lentigines, bilateral mild hearing loss, cardiac anomalies, ECG abnormalities, short stature, and apparent ocular hypertelorism. His early developmental milestones are not well known. He has been noted to have obsession with a specific topic, repetitive routine and rituals, and clumsy movements. At age 50 years, his social skills and aggressive behavior were noted to be deteriorating, and consequently he was suspected of having Asperger's disorder based on DSM-IV-TR. He met the diagnostic criteria of Asperger's disorder with Category 1 (1 and 3), Category 2 (1 and 2), and the rest of the four categories. His ASSQ score was 20 at age 55 years by his wife's evaluation. He has the same heterozygous *PTPN11* mutation (Table 1).

3. Discussion

The presented familial case of LEOPARD syndrome included individuals (patients 1, 2, and 4) diagnosed with or suspected of having Asperger's disorder, and

Table 1
Summary of clinical findings and *PTPN11* mutation.

	Pt. 1 Male	Pt. 2 Male	Pt. 3 Male	Pt. 4Male
Age	20 y	15 y	22 y	55 y
Physical findings				
Skin: café-au-lait spots	multiple	a few	a few	a few
Lentigines	+++	+++	-	+++
Cardiac defects	VSD	No	No	No
EKG abnormalities	+	No	WPW	No
Ocular hypertelorism	+	+	+	+
Pulmonary stenosis	No	No	No	No
Abnormal genitalia	No	Und. Testes*	Und. Testes*	No
Renal anomalies	R-hypoplasia	No	No	No
Retardation of growth	Yes	+	+	No
Deafness	No	No	No	Yes
Miscellaneous:				
Rocker bottom feet	Yes	Yes	Yes	No
Macrocephaly	Yes	Yes	Yes	No
PTPN11 mutation	T468 M	T468 M	T468 M	T468 M
Neuropsychological				
Diagnosis	AD**	AD**	PDDNOS***	AD**
ASSQ score[1] (age)	41 (12 y)	32 (15 y)	7 (22 y)	20 (50 y)
WISC-III[2] (age)	85 (12 y)	99 (9 y)	n/a	n/a
-Verbal/performance	77/98	104/92	n/a	n/a

* Und. Testes, undescended testes.
** AD, Asperger's disorder.
*** PDDNOS, Pervasive developmental disorder not otherwise specified.
[1] ASSQ score, Autism Spectrum Screening Questionnaire Score. The cutoff score of 3 predicts 91% of the true positive rate of Autistic spectrum disorders.
[2] WISC-III, Wechsler Intelligence Scale for Children-third edition.

patient 3 was diagnosed as having PDDNOS, which may lead to the diagnosis of ASD. ASDs were first introduced by Lorna Wing, who suggested that Asperger's disorder is a type of ASD and described in detail its various manifestations in speech, nonverbal communication, social interaction, motor coordination, motor clumsiness, and idiosyncratic interests [3]. Patient 3 did not have enough clinical symptoms to meet the diagnostic criteria for Asperger's disorder; however, he had some symptoms suggestive of ASD in his childhood that led to a diagnosis of PDDNOS.

The ASSQ is a 27-item checklist for completion by lay informants when assessing characteristic symptoms of Asperger's disorder and high-functioning autism in children and adolescents with normal intelligence or mild mental retardation. The ASSQ allows for rating on a 3-point scale (0, 1, or 2; 0 indicating normality, 1 some abnormality, and 2 definite abnormality). The range of possible scores is 0–54. The mean ASSQ parent scores in the Asperger's disorder validation sample were 25.1 (SD, 7.3) [14]. The cutoff score of 13 is 91% of the true positive rate of ASDs. The ASSQ score was established as a screening tool primarily for children between 6 and 17 years of age by parents and/or teachers. The delayed evaluation of patient 3 may account for the difference in diagnosis between this patient and his siblings.

ASDs are known to be associated with particular genetic disorders such as fragile X syndrome [10,15, 16], tuberous sclerosis (TSC) [7], and neurofibromatosis type 1 [8,9]. Fifty percent of children with TSC have behavioral problems in the form of ASDs. Gene mutations in either *TSC1* or *TSC2* influence neural precursors, resulting in abnormal cell differentiation and dysregulated control of cell size. These cells migrate to the cortex to generate an abnormal collection of inappropriately positioned neurons, causing widespread cortical disorganization and structural abnormalities [7]. Mutations in *PTPN11* causing LEOPARD syndrome induce catalytically impaired Shp2. In situ hybridization detected Shp2 expression in the neural ectoderm and nervous system in mouse embryos, suggesting an involvement of Shp2 in neural development. Shp2 is a critical signaling molecule in the coordinated regulation of progenitor cell proliferation and neuronal/astroglial cell differentiation. The studies with mutant mouse strains with Shp2 selectively deleted in neural precursor cells showed a dramatic phenotype of growth retardation, early postnatal lethality, and multiple defects in proliferation and cell fate specification in neural stem/progenitor cells [17]. The product of the TSC2 gene tuberin is known to up-regulate the B-RAF/MEK/MAPK signal transduction pathway. B-RAF is required for neuronal differentiation, suggesting another possible link between B-RAF signaling and the clinical manifestations of TSC including ASDs [18]. Disturbed neuronal cell differentiation and development due to mutations in

the TSC genes and the *PTPN11* gene are likely to contribute to the development of ASDs in patients with these syndromes.

NF-1 is well known to be associated with ASDs. The prevalence of autism in patients with NF-1 was reported to be 4% [9]. The well-known function of the NF-1 protein is to act as a RAS-GTPase-activating protein known to be involved in the regulation of the RAS-mitogen-activated protein kinase (MAPK) pathway. Mutations in the NF-1 gene are thought to result in activation of the RAS/MAPK signal transduction pathway [2]. Clinical overlap between LEOPARD syndrome and NF-1 is also well known [19].

Approximately 50% of patients with Noonan syndrome are due to missense *PTPN11* mutations [20]. *PTPN11* encodes SHP2, a protein tyrosine phosphatase, that is involved in the activation of the RAS/MAPK cascade [2]. Noonan syndrome is caused by "gain of function" *PTPN11* mutations [1,2], and the SHP2 mutants due to the *PTPN11* mutations causing Noonan syndrome cause prolonged activation of the RAS/MAPK pathway [2]. Schubbert et al. [21] reported that germline KRAS mutations cause Noonan syndrome through the hyperactive RAS/MAPK pathway.

Herault et al. [22] reported a positive association of the HRAS gene and autism. The psychological profiles of adults and children with Noonan syndrome have been studied, and deficiencies in social and emotional recognition and expression have been identified in adults, while low verbal IQ, clumsiness, and impairment of developmental coordination have been reported in children [23].

To date, there have been no reports to suggest an association of LEOPARD syndrome and ASDs. Our observations in this familial case may suggest at least some degree of association between LEOPARD syndrome and ASD phenotypes possibly through the RAS/MAPK signal transduction pathway. Further studies with more patients with LEOPARD syndrome are needed to establish the association and to investigate the genetic contributing factors causing ASDs, leading to the prevention and earlier detection of ASDs and better management of patients with these disorders.

References

[1] Kontaridis M, Swanson KD, David FS, Barford D, Neel BG. PTPN11 (Shp2) mutations in LEOPARD syndrome have dominant negative, not activating, effects. J Biol Chem 2006;281:6785–92.

[2] Aoki Y, Niihori T, Narumi Y, Kure S, Matsubara Y. The RAS/MAPK syndromes:novel roles of the RAS pathway in human genetic disorders. Hum Mutat 2008;29:992–1006.

[3] Wing L. Autistic spectrum disorders. BMJ 1996;312:327–8.

[4] Khouzam HR, El-Gabalawi F, Pirwani N, Priest F. Asperger's disorder: a review of its diagnosis and treatment. Comp Psychiatr 2004;45:181–91.

[5] American Psychiatric Association. Diagnostic and Statistical Manual of Mental Disorders. 4th ed.-Text Revision. Washington, DC: American Psychiatric Association; 2000.

[6] Muhle R, Trentacose SV, Rapin I. The genetics of autism. Pediatrics 2004;113:e472–86.

[7] Curatolo P. Tuberous sclerosis: genes, brain, and behavior. Dev Med Child Neurol 2006;48:404.

[8] Gillberg C, Forsell C. Childhood psychosis and neurofibromatosis-More than a coincidence? J Autism Dev Disord 1984;14:1–8.

[9] Williams PG, Hersh JH. The association of neurofibromatosis Type I and autism. J Autism Dev Disord 1998;28:567–71.

[10] Cohen IL, Sudhalter V, Pfadt A, Jenkins EC, Brown WT, Vietze PM. Why are autism and the fragile-X syndrome associated? Conceptual and methodological issues. Am J Hum Genet 1991;48:195–202.

[11] Verhoeven W, Wingbermuhle E, Egger J, Van der Burgt I, Tuinier S. Noonan syndrome: psychological and psychiatric aspects. Am J Med Genet A 2008;146A:191–6.

[12] Ghaziuddin M, Bolyard B, Alessi N. Autistic disorder in Noonan syndrome. J Intell Disabil Res 1994;38:67–72.

[13] Niihori T, Aoki Y, Ohashi H, Kurosawa K, Kondoh T, Ishikiriyama S, et al. Functional analysis of PTPN11/SHP-2 mutants identified in Noonan syndrome and childhood leukemia. J Hum Genet 2005;50:192–202.

[14] Ehlers S, Gillberg C, Wing L. A screening questionnaire for Asperger syndrome and other high-functioning autism spectrum disorders in school age children. J Autism Dev Disord 1999;29:129–41.

[15] Wahlstrom J, Gillberg C, Gustavson KH, Holmgren G. A Swedish multicenter study. Am J Med Genet 1986;23:403–8.

[16] Tranebjaerg L, Kure P. Prevalence of fra (X) and other specific diagnoses in autistic individuals in a Danish county. Am J Med Genet 1991;38:212–4.

[17] Ke Y, Zhang EE, Hagihara K, Wu D, Pang Y, Klein R, et al. Deletion of Shp2 in the brain leads to defective proliferation and differentiation in neural stem cells, and early postnatal lethality. Mol Cell Biol 2007;27:6706–17.

[18] Karbowniczek M, Cash T, Cheung M, Robertson GP, Astrinidis A, Henske EP. Regulation of B-Raf kinase activity by Tuberin and Rheb is mammalian target of Rapamycin (mTOR)-independent. J Biol Chem 2004;279:29930–7.

[19] Sarkozy A, Conti E, Digilio MC, Marino B, Morini E, Pacileo G, et al. J Med Genet 2004;41:e68.

[20] Tartaglia M, Mehler EL, Goldberg R, Zampino G, Brunner HG, Kremer H, et al. Mutations in PTPN11, encoding the protein tyrosine phosphatase SHP-2, cause Noonan syndrome. Nat Genet 2001;29:465–8.

[21] Schubbert S, Zenker M, Rowe SL, Boll S, Klein C, Bollag G, et al. Germline KRAS mutations cause Noonan syndrome. Nat Genet 2006;38:331–6.

[22] Herault J, Petit E, Martineau J, Perrot A, Lenoir P, Cherpi C, et al. Autism and genetics: clinical approach and association study with two markers of HRAS gene. Am J Med Genet 1995;60:276–81.

[23] Lee DA, Portnoy S, Hill P, Gillberg C, Patton MA. Psychological profile of children with Noonan syndrome. Dev Med Child Neurol 2005;47:35–8.

Journal of Human Genetics (2011) 56, 34–40

www.nature.com/jhg

ORIGINAL ARTICLE

A genome-wide association study identifies *RNF213* as the first Moyamoya disease gene

Fumiaki Kamada[1], Yoko Aoki[1], Ayumi Narisawa[1,2], Yu Abe[1], Shoko Komatsuzaki[1], Atsuo Kikuchi[3], Junko Kanno[1], Tetsuya Niihori[1], Masao Ono[4], Naoto Ishii[5], Yuji Owada[6], Miki Fujimura[2], Yoichi Mashimo[7], Yoichi Suzuki[7], Akira Hata[7], Shigeru Tsuchiya[3], Teiji Tominaga[2], Yoichi Matsubara[1] and Shigeo Kure[1,3]

Moyamoya disease (MMD) shows progressive cerebral angiopathy characterized by bilateral internal carotid artery stenosis and abnormal collateral vessels. Although ~15% of MMD cases are familial, the MMD gene(s) remain unknown. A genome-wide association study of 785 720 single-nucleotide polymorphisms (SNPs) was performed, comparing 72 Japanese MMD patients with 45 Japanese controls and resulting in a strong association of chromosome 17q25-ter with MMD risk. This result was further confirmed by a locus-specific association study using 335 SNPs in the 17q25-ter region. A single haplotype consisting of seven SNPs at the *RNF213* locus was tightly associated with MMD ($P=5.3\times10^{-10}$). *RNF213* encodes a really interesting new gene finger protein with an AAA ATPase domain and is abundantly expressed in spleen and leukocytes. An RNA *in situ* hybridization analysis of mouse tissues indicated that mature lymphocytes express higher levels of *Rnf213* mRNA than their immature counterparts. Mutational analysis of *RNF213* revealed a founder mutation, p.R4859K, in 95% of MMD families, 73% of non-familial MMD cases and 1.4% of controls; this mutation greatly increases the risk of MMD ($P=1.2\times10^{-43}$, odds ratio=190.8, 95% confidence interval=71.7–507.9). Three additional missense mutations were identified in the p.R4859K-negative patients. These results indicate that *RNF213* is the first identified susceptibility gene for MMD.
Journal of Human Genetics (2011) **56**, 34–40; doi:10.1038/jhg.2010.132; published online 4 November 2010

INTRODUCTION

'Moyamoya' is a Japanese expression for something hazy, such as a puff of cigarette smoke drifting in the air. In individuals with Moyamoya disease (MMD), there is a progressive stenosis of the internal carotid arteries; a fine network of collateral vessels, which resembles a puff of smoke on a cerebral angiogram, develops at the base of the brain (Figure 1a).[1,2] This steno-occlusive change can cause transient ischemic attacks and/or cerebral infarction, and rupture of the collateral vessels can cause intracranial hemorrhage. Children under 10 years of age account for nearly 50% of all MMD cases.[3]

The etiology of MMD remains unclear, although epidemiological studies suggest that bacterial or viral infection may be implicated in the development of the disease.[4] Growing attention has been paid to the upregulation of arteriogenesis and angiogenesis associated with MMD because chronic ischemia in other disease conditions is not always associated with a massive development of collateral vessels.[5,6] Several angiogenic growth factors are thought to have functions in the development of MMD.[7]

Several lines of evidence support the importance of genetic factors in susceptibility to MMD.[8] First, 10–15% of individuals with MMD have a family history of the disease.[9] Second, the concordance rate of MMD in monozygotic twins is as high as 80%.[10] Third, the prevalence of MMD is 10 times higher in East Asia, especially in Japan (6 per 100 000 population), than in Western countries.[3] Familial MMD may be inherited in an autosomal dominant fashion with low penetrance or in a polygenic manner.[11] Linkage studies of MMD families have revealed five candidate loci for an MMD gene: chromosomes 3p24–26,[12] 6q25,[13] 8q13–24,[10] 12p12–13[10] and 17q25.[14] However, no susceptibility gene for MMD has been identified to date.

We collected 20 familial cases of MMD to investigate linkage in the five putative MMD loci. However, a definitive result was not obtained for any of the loci. We then hypothesized that there might be a founder mutation among Japanese patients with MMD because the prevalence of MMD is unusually high in Japan.[15] Genome-wide and locus-specific association studies were performed and successfully identified a single gene, *RNF213*, linked to MMD. We report here a strong association between MMD onset and a founder mutation in *RNF213*, as well as the expression profiles of *RNF213*, in various tissues.

[1]Department of Medical Genetics, Tohoku University School of Medicine, Sendai, Japan; [2]Department of Neurosurgery, Tohoku University School of Medicine, Sendai, Japan; [3]Department of Pediatrics, Tohoku University School of Medicine, Sendai, Japan; [4]Department of Pathology, Tohoku University School of Medicine, Sendai, Japan; [5]Department of Microbiology and Immunology, Tohoku University School of Medicine, Sendai, Japan; [6]Department of Organ Anatomy, Yamaguchi University Graduate School of Medicine, Ube, Japan and [7]Department of Public Health, Graduate School of Medicine, Chiba University, Chiba, Japan
Correspondence: Dr S Kure, Department of Pediatrics, Tohoku University School of Medicine, 1-1 Seiryo-machi, Aoba-ku, Miyagi, Sendai 980-8574, Japan.
E-mail; kure@med.tohoku.ac.jp
Received 30 September 2010; accepted 1 October 2010; published online 4 November 2010

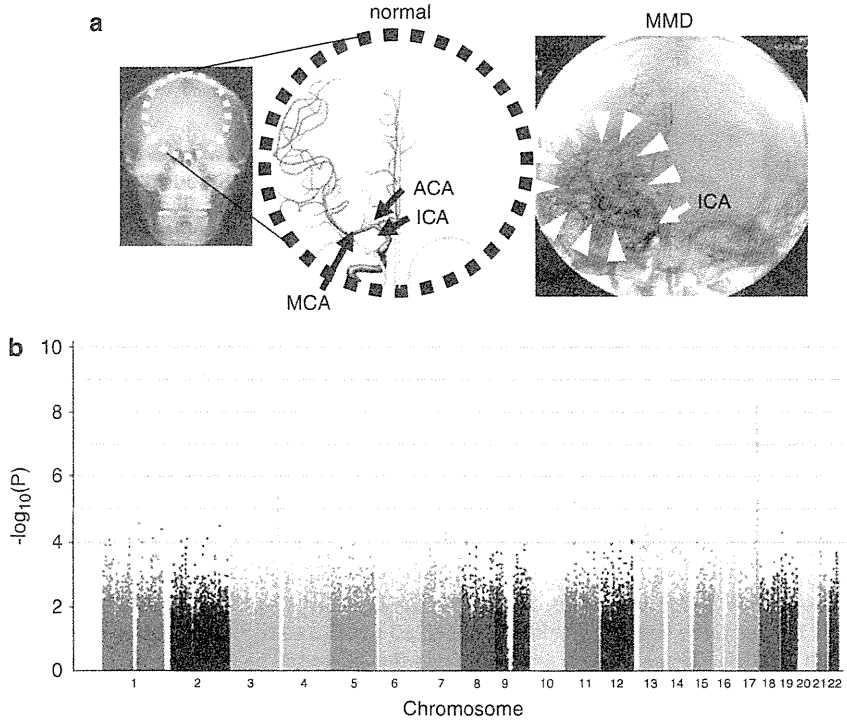

Figure 1 (a) Abnormal brain vessels in MMD. The dotted circle indicates the X-ray field of cerebral angiography (left panel). Normal structures of the right internal carotid artery (ICA), anterior cerebral artery (ACA) and middle cerebral artery (MCA) are illustrated (middle panel). The arrowheads indicate abnormal collateral vessels appearing like a puff of smoke in the angiogram of an individual with MMD (right panel). Note that ACA and MCA are barely visible, because of the occlusion of the terminal portion of the ICA. (b) Manhattan plot of the 785 720 SNPs used in the genome-wide association analysis of MMD patients. Note that the SNPs in the 17q25-ter region reach a significance of $P<10^{-8}$.

MATERIALS AND METHODS

Affected individuals

Genomic DNA was extracted from blood and/or saliva samples obtained from members of the families with MMD (Supplementary Figure 1), MMD patients with no family history and control subjects. All of the subjects were Japanese. MMD was diagnosed on the basis of guidelines established by the Research Committee on Spontaneous Occlusion of the Circle of Willis of the Ministry of Health and Welfare of Japan. This study was approved by the Ethics Committee of Tohoku University School of Medicine. Total RNA samples were purified from leukocytes using an RNeasy mini kit (Qiagen, Hilden, Germany) and used as templates for cDNA synthesis with an Oligo $(dT)_{20}$ primer and SuperScript II reverse transcriptase according to the manufacturer's instructions (Invitrogen, Carlsbad, CA, USA).

Linkage analysis

For the linkage analysis, DNA samples were genotyped for 36 microsatellite markers within five previously reported MMD loci using the ABI 373A DNA Sequencer (Applied Biosystems, Foster City, CA, USA). Pedigrees and haplotypes were constructed with the Cyrillic version 2.1 software (Oxfordshire, UK). Multipoint analyses were conducted using the GENEHUNTER 2 software (http://www.broadinstitute.org/ftp/distribution/software/genehunter/). Statistical analysis was performed with SPSS version 14.0J (SPSS, Tokyo, Japan).

Genome-wide and locus-specific association studies

A genome-wide association study was performed using a group of 72 MMD patients, which consisted of 64 patients without a family history of MMD and 8 probands of MMD families. The Illumina Human Omni-Quad 1 chip (Illumina, San Diego, CA, USA) was used for genotyping, and single-nucleotide polymorphisms (SNPs) with a genotyping completion rate of 100% were used for further statistical analysis (785 720 out of 1 140 419 SNPs). Genotyping data from 45 healthy Japanese controls were obtained from the database at the International HapMap Project web site. The 785 720 SNPs were statistically analyzed using the PLINK software (http://pngu.mgh.harvard.edu/~purcell/plink/index.shtml). For a locus-specific association study, we used 63 DNA samples consisting of 58 non-familial MMD patients and 5 probands of MMD families. A total of 384 SNPs within chromosome 17q25-ter were genotyped (Supplementary Table 1), using the GoldenGate Assay and a custom SNP chip (Illumina). Genotyping data for 45 healthy Japanese were used as a control. Case–control single-marker analysis, haplotype frequency estimation and significance testing of differences in haplotype frequency were performed using the Haploview version 3.32 program (http://www.broad.mit.edu/mpg/haploview/).

Mutation detection

Mutational analyses of *RNF213* and *FLJ35220* were performed by PCR amplification of each coding exon and putative promoter regions, followed by direct sequencing. Genomic sequence data for the two genes were obtained from the National Center for Biotechnology Information web site (http://www.ncbi.nlm.nih.gov/) for design of exon-specific PCR primers. *RNF213* cDNA fragments were amplified from leukocyte mRNA for sequencing analysis. Sequencing of the PCR products was performed with the ABI BigDye Terminator Cycle Sequencing Reaction Kit using the ABI 310 Genetic Analyzer. Identified base changes were screened in control subjects. Statistical difference of the carrier frequency of each base change was estimated by Fisher's exact test (the MMD group vs the control group).

Quantitative PCR

MTC Multiple Tissue cDNA Panels (Clontech Laboratory, Madison, WI, USA) were the source of cDNAs from human cell lines, adult and fetal tissues. Mononuclear cells and polymorphonuclear cells were isolated from the fresh peripheral blood of healthy human adults using Polymorphprep (Cosmo Bio,

Carlsbad, CA, USA). T and B cells were isolated from the fresh peripheral blood of healthy human adults using the autoMACS separator (Militeny Biotec, Bergisch Gladbach, Germany). Total RNA was isolated from these cells with the RNeasy Mini Kit (Qiagen) following the manufacturer's instructions. We reverse transcribed 100 ng samples of total RNA into cDNAs using the High Capacity cDNA Reverse Transcription Kit (Applied Biosystems). Quantitative PCRs were performed in a final volume of 20 µl using the FastStart TaqMan Probe Master (Rox) (Roche, Madison, WI, USA), 5 µl of cDNA, 10 µM of *RNF*- or *GAPDH*-specific primers and 10 µM of probes (Universal ProbeLibrary Probe #80 for *RNF213* and Roche Probe #60 for *GAPDH*). All reactions were performed in triplicate using the ABI 7500 Real-Time PCR system (Applied Biosystems). Cycling conditions were 2 min at 50°C and 10 min at 95°C, followed by 40 cycles of 15 s at 95°C and 60 s at 60°C. Real-time PCR data were analyzed by the SDS version 1.2.1 software (Applied Biosystems). We evaluated the relative level of *RNF213* mRNA by determining the C_T value, the PCR cycle at which the reporter fluorescence exceeded the signal baseline. *GAPDH* mRNA was used as an internal reference for normalization of the quantitative expression values.

Multiplex PCR

MTC Multiple Tissue cDNA Panels (Clontech) were the source of human cell lines and cDNAs from human adult and fetal tissues. Multiplex PCRs were performed in a final volume of 20 µl using the Multiplex PCR Master Mix (Qiagen), 2 µl of cDNA, a 2 µM concentration of *RNF213* and a 10 µM concentration of *GAPDH*-specific primers. The samples were separated on a 2% agarose gel stained with ethidium bromide. Cycling conditions were 15 min at 94°C, followed by 30 cycles of 30 s at 94 °C, 30 s at 57 °C and 30 s at 72 °C. For normalization of the expression levels, we used *GAPDH* as an internal reference for each sample.

In situ hybridization (ISH) analysis

Paraffin-embedded blocks and sections of mouse tissues for ISH were obtained from Genostaff (Tokyo, Japan). The mouse tissues were dissected, fixed with Tissue Fixative (Genostaff), embedded in paraffin by proprietary procedures (Genostaff) and sectioned at 6 µm. To generate anti-sense and sense RNA probes, a 521-bp DNA fragment corresponding to nucleotide positions 470–990 of mouse *Rnf213* (BC038025) was subcloned into the pGEM-T Easy vector (Promega, Madison, WI, USA). Hybridization was performed with digoxigenin-labeled RNA probes at concentrations of 300 ng ml^{-1} in Probe Diluent-1 (Genostaff) at 60 °C for 16 h. Coloring reactions were performed with NBT/BCIP solution (Sigma-Aldrich, St Louis, MO, USA). The sections were counterstained with Kernechtrot stain solution (Mutoh, Tokyo, Japan), dehydrated and mounted with Malinol (Mutoh). For observation of *Rnf213* expression in activated lymphocytes, 10-week-old Balb/c mice were intraperitoneally injected with 100 µg of keyhole limpet hemocyanin and incomplete adjuvant and sacrificed in 2 weeks. The spleen of the mice was removed for Hematoxylin–eosin staining and ISH analyses.

RESULTS

Using 20 Japanese MMD families, we reevaluated the linkage mapped previously to five putative MMD loci. No locus with significant linkage, Lod score >3.0 or NPL score >4.0 was confirmed (Supplementary Figure 2). We conducted a genome-wide association study of 72 Japanese MMD cases. Single-marker allelic tests comparing the 72 MMD cases and 45 controls were performed for 785 720 SNPs using χ^2 statistics. These tests identified a single locus with a strong association with MMD ($P<10^{-8}$) on chromosome 17q25-ter (Figure 1b), which is in line with the latest mapping data of a MMD locus.[16] The SNP markers with $P<10^{-6}$ are listed in Table 1. To confirm this observation, we performed a locus-specific association study. A total of 384 SNP markers (Supplementary Table 1) were selected within the chromosome 17q25-ter region and genotyped in a set of 63 MMD cases and 45 controls. The SNP markers demonstrating a high association with MMD ($P<10^{-6}$) were clustered in a 151-kb region from base position 75 851 399–76 003 020 (SNP No.116–136 in

Table 1 A genome-wide association study of Japanese MMD patients and controls

	SNP	Chromosome	Base position	Gene	Risk allele/ non-risk allele	Risk allele frequency in MMD	Risk allele frequency in controls	χ^2	P-value	Odds ratio	95% confidence interval	
											Lower	Upper
1	rs11870849	17	76 025 668	*RNF213*	T/C	0.4792	0.1111	33.55	6.95E-09	7.36	3.532	15.34
2	rs6565681	17	75 963 089	*RNF213*	A/G	0.7361	0.3667	31.35	2.16E-08	4.819	2.733	8.489
3	rs7216493	17	75 941 953	*RNF213*	G/A	0.75	0.3889	30.39	3.53E-08	4.715	2.673	8.313
4	rs7217421	17	75 850 055	*RNF213*	A/G	0.6667	0.3	29.86	4.64E-08	4.666	2.642	8.237
5	rs12449863	17	75 857 806	*RNF213*	C/T	0.6667	0.3	29.86	4.64E-08	4.666	2.642	8.237
6	rs4890009	17	75 926 103	*RNF213*	G/A	0.8819	0.5778	28.5	9.38E-08	5.459	2.831	10.527
7	SNP17-75933731	17	75 933 731	*RNF213*	G/A	0.8819	0.5778	28.5	9.38E-08	5.458	2.831	10.527
8	rs7219131	17	75 867 365	*RNF213*	T/C	0.6667	0.3111	28.11	1.15E-07	4.429	2.517	7.794
9	rs6565677	17	75 932 037	*RNF213*	T/C	0.7431	0.3977	27.43	1.63E-07	4.378	2.483	7.722
10	rs4889848	17	75 969 256	*RNF213*	C/T	0.75	0.4111	26.99	2.05E-07	4.297	2.444	7.889
11	rs7224239	17	75 969 771	*RNF213*	A/G	0.8681	0.5667	26.99	2.05E-07	5.03	2.659	9.529

Abbreviations: MMD, moyamoya disease; SNP, single-nucleotide polymorphism.A genome-wide association study testing 1 140 419 SNPs on the Human Omni-Quad 1chip (Illumina, San Diego, CA, USA) was performed in 72 Japanese MMD cases. Single-marker allelic tests between the cases and controls were performed using χ^2 statistics for all markers. This table lists the 11 SNP markers with a significance of $P<10^{-6}$.

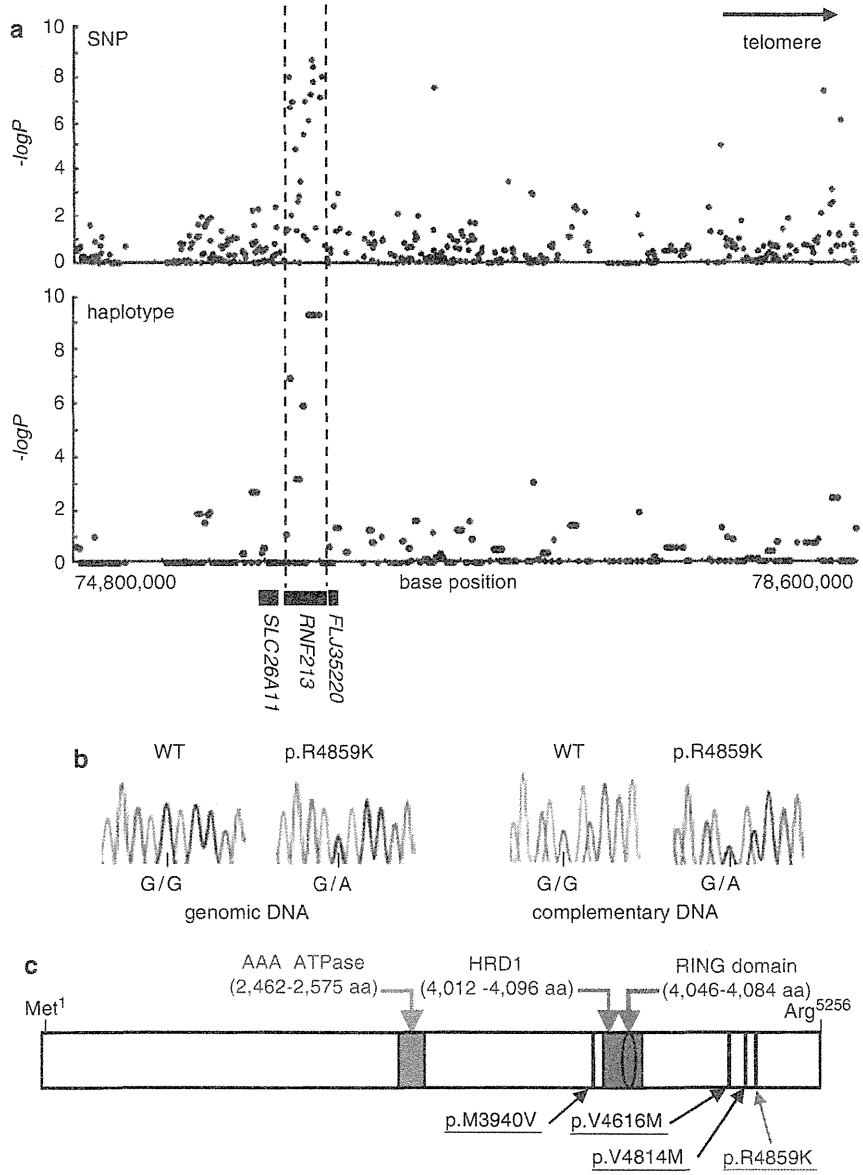

Figure 2 (**a**) Association analysis of 63 non-familial MMD cases and 45 control subjects. Statistical significance was evaluated by the χ^2-test. SNP markers with a strong association with MMD ($P<10^{-6}$) clustered in a 161-kb region (base position 75 851 399–76 012 838) indicated by two dotted lines (upper panel), which included the entire region of *RNF213* (lower panel). Haplotype analysis revealed a strong association ($P=5.3\times10^{-10}$) between MMD and a single haplotype located within *RNF213*. (**b**) Sequencing chromatograms of the identified MMD mutations. The left panel shows the sequences of an unaffected individual and a carrier of a p.R4859K heterozygous mutation. The right panel indicates the sequencing chromatograms of the leukocyte cDNA obtained from an unaffected individual and an individual with MMD who carries the p.R4859K mutation. Note that both wild-type and mutant alleles were expressed in leukocytes. (**c**) The structure of the RNF213 protein. The RNF213 protein contains three characteristic structures, the AAA-superfamily ATPase motif, the RING motif and the HMG-CoA reductase degradation motif. The positions of four mutations identified in MMD patients are underlined, including one prevalent mutation (red) and three private mutations (black).

Supplementary Table 1); this entire region was within the *RNF213* locus (Figure 2a). A single haplotype determined by seven SNPs (SNP Nos.130–136 in Supplementary Table 1) that resided in the 3′ region of *RNF213* was strongly associated with MMD onset ($P=5.3\times10^{-10}$). Analysis of the linkage disequilibrium block indicated that this haplotype was not in complete linkage disequilibrium with any other haplotype in this region (Supplementary Figure 3). These results strongly suggest that a founder mutation may exist in the 3′ part of *RNF213*.

Mutational analysis of the entire coding and promoter regions of *RNF213* and *FLJ35220*, a gene 3′ adjacent to *RNF213*, revealed that 19 of the 20 MMD families shared the same single base substitution, c.14576G>A, in exon 60 of *RNF213* (Figure 2b and Table 2). This nucleotide change causes an amino-acid substitution from arginine^{4859} to lysine^{4859} (p.R4859K). The p.R4859K mutation was identified in 46 of 63 non-familial MMD cases (73%), including 45 heterozygotes and a single homozygote (Table 3). Both the wild-type and the p.R4859K mutant alleles were co-expressed in leukocytes

Table 2 Nucleotide changes with amino-acid substitutions identified in the sequencing analysis of *RNF213* and *FLJ35220*

			Genotype (allele)				
Gene	*Exon*	*Nucleotide change[a] (amino-acid substitution)*	*Non-familial cases*	*Control subjects*	*P-value[b]*	*χ^2 (df=1) [c]*	*Odds ratio (95% CI)*
RNF213	29	c.7809C>A (p.D2603E)	2/63 (2/126)	15/381 (15/762)	0.77	0.09	0.80 (0.2–3.6)
RNF213	41	c.11818A>G (p.M3940V)	1/63 (1/126)	0/388 (0/776)	0.01	6.17	ND
RNF213	41	c.11891A>G (p.E3964G)	4/63 (4/126)	3/55 (4/110)	0.84	0.04	1.2 (0.3–5.5)
RNF213	52	c.13342G>A (p.A4448T)	4/63 (4/126)	2/53 (2/106)	0.53	0.39	1.7 (0.3–9.8)
RNF213	56	c.13846G>A (p.V4616M)	1/63 (1/126)	0/388 (0/776)	0.01	6.17	ND
RNF213	59	c.14440G>A (p.V4814M)	1/63 (1/126)	0/388 (0/776)	0.01	6.17	ND
RNF213	60	c.14576G>A (p.R4859K)	46/63 (47/126)	6/429 (6/858)	1.2×10^{-43}	298.1	190.8 (71.7–507.9)
FLJ35220		None					

Abbreviations: ND, not determined; SNP, single-nucleotide polymorphism.
[a]Nucleotide numbers of *RNF213* cDNA are counted from the A of the ATG initiator methionine codon (NCBI Reference sequence, NP_065965.4).
[b]*P*-values were calculated by Fisher's exact test.
[c]Genotypic distribution (carrier of the polymorphism vs non-carrier).

Table 3 Association of the p.R4859K (c.14576G>A) mutation with MMD

		Genotype		
	Total	*wt/wt (%)*	*wt/p.R4859K (%)*	*p.R4859K/ p.R4859K (%)[d]*
Members of 19 MMD families[a]				
Affected	42	0	39 (92.9)	3 (7.1)
Not affected	28	15 (53.6)	13 (46.4)	0
Individuals without a family history of MMD[b,c]				
Affected	63	17 (27.0)	45 (71.4)	1 (1.6)
Not affected	429	423 (98.6)	6 (1.4)	0

Abbreviations: MMD, moyamoya disease.
[a]Entire distribution, $\chi^2=29.4$, $P=4.2\times10^{-7}$.
[b]Entire distribution, $\chi^2=298.2$, $P=1.8\times10^{-65}$.
[c]Genotypic distribution (p.R4859K carrier vs non-carrier), $\chi^2=298.1$, $P=1.2\times10^{-43}$, odds ratio=190.8 (95% CI=71.7–507.9).
[d]The age of onset and initial symptoms of the four homozygotes were comparable to those of the 84 heterozygous patients.

in three patients heterozygous for the p.R4859K mutation (Figure 2b), excluding the possible instability of the mutant *RNF213* mRNA. Additional missense mutations, p.M3940V, p.V4616M and p.V4814M, were detected in three non-familial MMD cases without the p.R4859K mutation (Figure 2c). These mutations were not found in 388 control subjects and were detected in only one patient, suggesting that they were private mutations (Table 2). No copy number variation or mutation was identified in the *RNF213* locus of 12 MMD patients using comparative genome hybridization microarray analysis (Supplementary Figure 4). In total, 6 of the 429 control subjects (1.4%) were found to be heterozygous carriers of p.R4859K. Therefore, we concluded that the p.R4859K mutation increases the risk of MMD by a remarkably high amount (odds ratio=190.8 (95% confidence interval=71.7–507.9), $P=1.2\times10^{-43}$) (Table 3). It was recently reported that an SNP (ss161110142) in the promoter region of *RPTOR*, which is located ~150 kb downstream from *RNF213*, was associated with MMD.[17] Genotyping of the SNP in *RPTOR* showed that the *RNF213* p.R4859K mutation was more strongly associated with MMD than ss161110142 (Supplementary Figure 1).

RNF213 encodes a protein with 5256 amino acids harboring a RING (really interesting new gene) finger motif, suggesting that it functions as an E3 ubiquitin ligase (Figure 2c). It also has an AAA ATPase domain, which is characteristic of energy-dependent unfoldases.[18] To our knowledge, RNF213 is the first RING finger protein known to contain an AAA ATPase domain. The expression profile of *RNF213* has not been previously fully characterized. We performed a quantitative reverse transcription PCR analysis in various human tissues and cells. *RNF213* mRNA was highly expressed in immune tissues, such as spleen and leukocytes (Figure 3a and Supplementary Figure 5). Expression of *RNF213* was detected in fractions of both polymorphonuclear cells and mononuclear cells and was found in both B and T cell fractions (Supplementary Figure 6). A low but significant expression of *RNF213* was also observed in human umbilical vein endothelial cells and human pulmonary artery smooth muscle cells. Cellular expression was not enhanced in tumor cell lines, compared with leukocytes. In human fetal tissues, the highest expression was observed in leukocytes and the thymus (Supplementary Figure 6E). The expression of *RNF213* was surprisingly low in both adult and fetal brains. Overall, *RNF213* was ubiquitously expressed, and the highest expression was observed in immune tissues.

We studied the cellular expression of *Rnf213* in mice. The ISH analysis of spleen showed that *Rnf213* mRNA was present in small mononuclear cells, which were mainly localized in the white pulps (Figures 3b–g). The ISH signals were also detected in the primary follicles in the lymph node and in thymocytes in the medulla of the thymus (Supplementary Figure 7). To study *Rnf213* expression in activated lymphocytes we immunized mice with keyhole limpet hemocyanin, and examined *Rnf213* mRNA in spleen by ISH analysis. Primary immunization with keyhole limpet hemocyanin antigen revealed that the expression of *Rnf213* in the secondary follicle is as high as in the primary follicle in the lymph node (Supplementary Figure 8). In an E16.5 mouse embryo, expression was observed in the medulla of the thymus and in the cells around the mucous palatine glands (Supplementary Figure 9). These findings suggest that mature lymphocytes in a static state express *Rnf213* mRNA at a higher level than do their immature counterparts.

DISCUSSION

We identified a susceptibility locus for MMD by genome-wide and locus-specific association studies. Further sequencing analysis revealed a founder missense mutation in *RNF213*, p.R4859K, which was tightly associated with MMD onset. Identification of a founder mutation in individuals with MMD would resolve the following recurrent

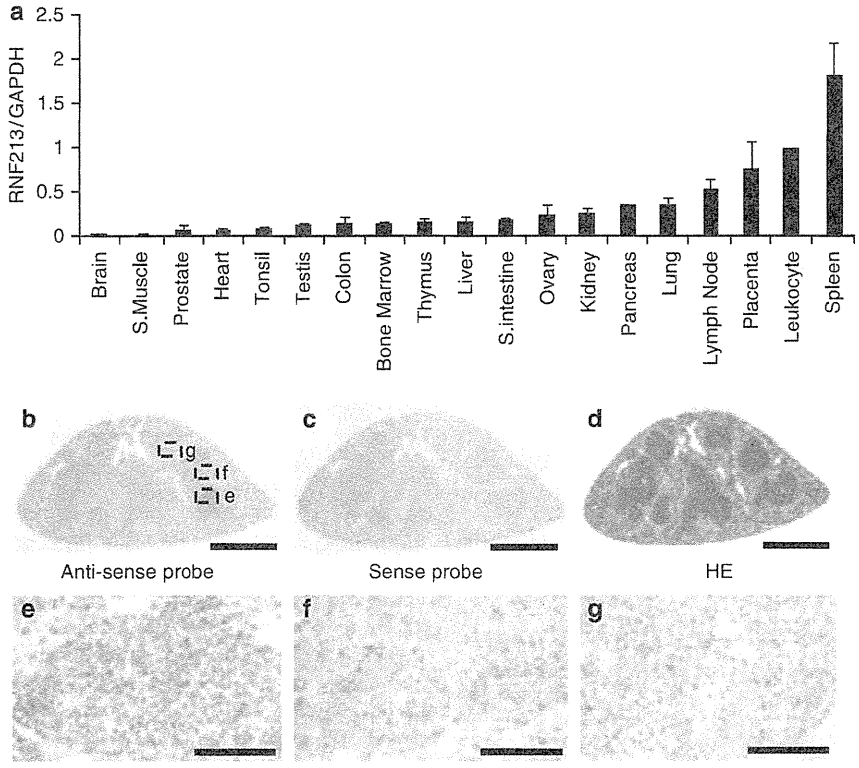

Figure 3 Expression of human RNF213 and murine Rnf213. (**a**) RT-PCR analysis of RNF213 mRNA in various human tissues. The expression levels of *RNF213* mRNA in various adult human tissues were evaluated by quantitative PCR using *GAPDH* mRNA as a control. The signal ratio of *RNF213* mRNA to *GAPDH* mRNA in each sample is shown on the vertical axis. (**b–g**) *In situ* hybridization (ISH) analysis of Rnf213 mRNA in mouse spleen. Specific signals for *Rnf213* mRNA were detected by ISH analysis with the anti-sense probe (**b**) but not with the sense probe (**c**). Hematoxylin–eosin staining of the mouse spleen (**d**). Signals for the *Rnf213* mRNA were observed in small mononuclear cells, which were mainly localized in the white pulps (dotted square, **e**) and partially distributed in the red pulps (dotted squares, **f** and **g**). Panels e, f and g show the high-magnification images of the corresponding fields in panel b. Scale bars, 1 mm (**b–d**) and 50 μm (**e–g**).

questions:[2,19] (i) why is MMD more prevalent in East Asia than in Western countries? The carrier frequency of p.R4859K in Japan is 1/72 (Table 2). In contrast, we found no p.R4859K carrier in 400 Caucasian controls (data not shown). Furthermore, no mutation was identified in five Caucasian patients with MMD after the full sequencing of *RNF213*. These results suggest that the genetic background of MMD in Asian populations is distinct from that in Western populations and that the low incidence of MMD in Western countries may be attributable to a lack of the founder *RNF213* mutation. (ii) Is unilateral involvement a subtype of MMD or a different disease?[2] We collected DNA samples from six patients with unilateral involvement and found a p.R4859K mutation in four of them (data not shown), suggesting that bilateral and unilateral MMD share a genetic background. (iii) Is pre-symptomatic diagnosis of MMD possible? In the present study, MMD never developed in the 15 mutation-negative family members in the 19 MMD families with the p.R4859K mutation (Table 3 and Supplementary Figure 1), suggesting the feasibility of presymptomatic diagnosis or exclusion by genetic testing.

How the mutant RNF213 protein causes MMD remains to be elucidated. The expression of *RNF213* was more abundant in a subset of leukocytes than in the brain, suggesting that blood cells have a function in the etiology of MMD. This observation agrees with a previous report that MMD patients have systemic angiopathy.[20] Recent studies have suggested that the postnatal vasculature can form through vasculogenesis, a process by which endothelial progenitor cell are recruited from the splenic pool and differentiate into mature endothelial cells.[21] Levels of endothelial progenitor cells in the peripheral blood are increased in MMD patients.[22] *RNF213* may be expressed in splenic endothelial progenitor cells and mutant *RNF213* might dysregulate the function of the endothelial progenitor cells. Further research is necessary to elucidate the role of *RNF213* in the etiology of MMD.

CONFLICT OF INTEREST

The authors declare no conflict of interest.

ACKNOWLEDGEMENTS

We thank all of the patients and their families for participating in this study. We also thank Dr Hidetoshi Ikeda at the Department of Neurosurgery, Tohoku University School of Medicine and Drs Toshiaki Hayashi and Reizo Shirane at the Department of Neurosurgery, Miyagi Children's Hospital, Sendai, Japan for patient recruitment. We are grateful to Ms Kumi Kato for technical assistance. This study was supported by grants from the Ministry of Education, Culture, Sports, Science and Technology, Japan and by the Research Committee on Moyamoya Disease of the Ministry of Health, Labor and Welfare, Japan.

1 Suzuki, J. & Takaku, A. Cerebrovascular 'moyamoya' disease. Disease showing abnormal net-like vessels in base of brain. *Arch. Neurol.* **20,** 288–299 (1969).
2 Suzuki, J. *Moyamoya Disease* (Springer-Verlag: Berlin, 1983).
3 Oki, K., Hoshino, H. & Suzuki, N. In: *Moyamoya Disease Update*, (eds Cho B.K., Tominaga T.) 29–34 (Springer: New York, 2010).
4 Phi, J. H., Kim, S. K., Wang, K. C. & Cho, B. K. In: *Moyamoya Disease Update*, (eds Cho B.K., Tominaga T). 82–86, (Springer: New York, 2010).
5 Yoshihara, T., Taguchi, A., Matsuyama, T., Shimizu, Y., Kikuchi-Taura, A., Soma, T. *et al.* Increase in circulating CD34-positive cells in patients with angiographic evidence of moyamoya-like vessels. *J. Cereb. Blood Flow Metab.* **28,** 1086–1089 (2008).
6 Achrol, A. S., Guzman, R., Lee, M. & Steinberg, G. K. Pathophysiology and genetic factors in moyamoya disease. *Neurosurg. Focus.* **26,** E4 (2009).
7 Scott, R. M. & Smith, E. R. Moyamoya disease and moyamoya syndrome.. *N. Engl. J. Med.* **360,** 1226–1237 (2009).
8 Kure, S. In: *Moyamoya Disease Update* (eds Cho B.K., Tominaga T.) 41–45 (Springer: Tokyo, 2010).
9 Kuriyama, S., Kusaka, Y., Fujimura, M., Wakai, K., Tamakoshi, A., Hashimoto, S. *et al.* Prevalence and clinicoepidemiological features of moyamoya disease in Japan: findings from a nationwide epidemiological survey. *Stroke.* **39,** 42–47 (2008).
10 Sakurai, K., Horiuchi, Y., Ikeda, H., Ikezaki, K., Yoshimoto, T., Fukui, M. *et al.* A novel susceptibility locus for moyamoya disease on chromosome 8q23. *J. Hum. Genet.* **49,** 278–281 (2004).
11 Nanba, R., Kuroda, S., Tada, M., Ishikawa, T., Houkin, K. & Iwasaki, Y. Clinical features of familial moyamoya disease. *Childs. Nerv. Syst.* **22,** 258–262 (2006).
12 Ikeda, H., Sasaki, T., Yoshimoto, T., Fukui, M. & Arinami, T. Mapping of a familial moyamoya disease gene to chromosome 3p24.2-p26. *Am. J. Hum. Genet.* **64,** 533–537 (1999).
13 Inoue, T. K., Ikezaki, K., Sasazuki, T., Matsushima, T. & Fukui, M. Linkage analysis of moyamoya disease on chromosome 6. *J. Child. Neurol.* **15,** 179–182 (2000).
14 Yamauchi, T., Tada, M., Houkin, K., Tanaka, T., Nakamura, Y., Kuroda, S. *et al.* Linkage of familial moyamoya disease (spontaneous occlusion of the circle of Willis) to chromosome 17q25.. *Stroke.* **31,** 930–935 (2000).
15 Wakai, K., Tamakoshi, A., Ikezaki, K., Fukui, M., Kawamura, T., Aoki, R. *et al.* Epidemiological features of moyamoya disease in Japan: findings from a nationwide survey. *Clin. Neurol. Neurosurg.* **99**(Suppl 2), S1–S5 (1997).
16 Mineharu, Y., Liu, W., Inoue, K., Matsuura, N., Inoue, S., Takenaka, K. *et al.* Autosomal dominant moyamoya disease maps to chromosome 17q25.3. *Neurology.* **70,** 2357–2363 (2008).
17 Liu, W., Hashikata, H., Inoue, K., Matsuura, N., Mineharu, Y., Kobayashi, H. *et al.* A rare Asian founder polymorphism of Raptor may explain the high prevalence of Moyamoya disease among East Asians and its low prevalence among Caucasians. *Environ. Health. Prev. Med.* **15,** 94–104 (2010).
18 Lupas, A. N. & Martin, J. AAA proteins.. *Curr. Opin. Struct. Biol.* **12,** 746–753 (2002).
19 Ikezaki, K. In: *Moyamoya disease* (eds Ikezaki K., Loftus C. M.) 43–75 (Thieme: New York, 2001).
20 Ikeda, E. Systemic vascular changes in spontaneous occlusion of the circle of Willis. *Stroke.* **22,** 1358–1362 (1991).
21 Zampetaki, A., Kirton, J. P. & Xu, Q. Vascular repair by endothelial progenitor cells. *Cardiovasc. Res.* **78,** 413–421 (2008).
22 Rafat, N., Beck, G., Pena-Tapia, P. G., Schmiedek, P. & Vajkoczy, P. Increased levels of circulating endothelial progenitor cells in patients with Moyamoya disease. *Stroke.* **40,** 432–438 (2009).

Supplementary Information accompanies the paper on Journal of Human Genetics website (http://www.nature.com/jhg)

Journal of Human Genetics (2011) 56, 91–93

www.nature.com/jhg

SHORT COMMUNICATION

Androgenetic/biparental mosaicism in a girl with Beckwith–Wiedemann syndrome-like and upd(14)pat-like phenotypes

Kazuki Yamazawa[1,5], Kazuhiko Nakabayashi[2], Kentaro Matsuoka[3], Keiko Masubara[1], Kenichiro Hata[2], Reiko Horikawa[4] and Tsutomu Ogata[1]

This report describes androgenetic/biparental mosaicism in a 4-year-old Japanese girl with Beckwith–Wiedemann syndrome (BWS)-like and paternal uniparental disomy 14 (upd(14)pat)-like phenotypes. We performed methylation analysis for 18 differentially methylated regions on various chromosomes, genome-wide microsatellite analysis for a total of 90 loci and expression analysis of *SNRPN* in leukocytes. Consequently, she was found to have an androgenetic 46,XX cell lineage and a normal 46,XX cell lineage, with the frequency of the androgenetic cells being roughly calculated as 91% in leukocytes, 70% in tongue tissues and 79% in tonsil tissues. It is likely that, after a normal fertilization between an ovum and a sperm, the paternally derived pronucleus alone, but not the maternally derived pronucleus, underwent a mitotic division, resulting both in the generation of the androgenetic cell lineage by endoreplication of one blastomere containing a paternally derived pronucleus and in the formation of the normal cell lineage by union of paternally and maternally derived pronuclei. It appears that the extent of overall (epi)genetic aberrations exceeded the threshold level for the development of BWS-like and upd(14)pat-like phenotypes, but not for the occurrence of other imprinting disorders or recessive Mendelian disorders.
Journal of Human Genetics (2011) **56,** 91–93; doi:10.1038/jhg.2010.142; published online 11 November 2010

Keywords: androgenesis; Beckwith–Wiedemann syndrome; mosaicism; upd(14)pat

INTRODUCTION

A pure androgenetic human with paternal uniparental disomy for all chromosomes is incompatible with life because of genomic imprinting.[1,2] However, a human with an androgenetic cell lineage could be viable in the presence of a normal cell lineage. Indeed, an androgenetic cell lineage has been identified in six liveborn individuals with variable phenotypes.[3–7] All the androgenetic cell lineages have a 46,XX karyotype, and this is consistent with the lethality of an androgenetic 46,YY cell lineage.

Here, we report on a girl with androgenetic/biparental mosaicism, and discuss the underlying factors for the phenotypic development.

CASE REPORT

This patient was conceived naturally to non-consanguineous and healthy parents. At 24 weeks gestation, the mother was referred to us because of threatened premature delivery. Ultrasound studies showed Beckwith–Wiedemann syndrome (BWS)-like features,[8] such as macroglossia, organomegaly and umbilical hernia, together with polyhydramnios and placentomegaly. The mother repeatedly received amnioreduction and tocolysis.

She was delivered by an emergency cesarean section because of preterm rupture of membranes at 34 weeks of gestation. Her birth weight was 3730 g (+4.8 s.d. for gestational age), and her length 45.6 cm (+0.7 s.d.). The placenta weighed 1040 g (+7.3 s.d.).[9] She was admitted to a neonatal intensive care unit due to asphyxia. Physical examination confirmed a BWS-like phenotype. Notably, chest roentgenograms delineated mild bell-shaped thorax characteristic of paternal uniparental disomy 14 (upd(14)pat),[10] although coat hanger appearance of the ribs indicative of upd(14)pat was absent (Supplementary Figure 1). She was placed on mechanical ventilation for 2 months, and received tracheostomy, glossectomy and tonsillectomy in her infancy, due to upper airway obstruction. She also had several clinical features occasionally reported in BWS[8] (Supplementary Table 1). Her karyotype was 46,XX in all the 50 lymphocytes analyzed. On the last examination at 4 years of age, she showed postnatal growth failure and severe developmental retardation.

[1]Department of Molecular Endocrinology, National Research Institute for Child Health and Development, Tokyo, Japan; [2]Department of Maternal-Fetal Biology, National Research Institute for Child Health and Development, Tokyo, Japan; [3]Division of Pathology, National Medical Center for Children and Mothers, Tokyo, Japan and [4]Division of Endocrinology and Metabolism, National Medical Center for Children and Mothers, Tokyo, Japan
[5]Current address: Department of Physiology, Development & Neuroscience, University of Cambridge, Cambridge, UK.
Correspondence: Dr T Ogata, Department of Molecular Endocrinology, National Research Institute for Child Health and Development, 2-10-1 Ohkura, Setagaya, Tokyo 157-8535, Japan.
E-mail: tomogata@nch.go.jp
Received 9 September 2010; revised 18 October 2010; accepted 22 October 2010; published online 11 November 2010

MOLECULAR STUDIES

This study was approved by the Institutional Review Board Committee at the National Center for Child health and Development, and performed after obtaining informed consent.

Methylation analysis

We first performed bisulfite sequencing for the *H19*-DMR (differentially methylated region) and KvDMR1 as a screening of BWS[11,12] and that for the IG-DMR and the *MEG3*-DMR as a screening of upd(14)pat,[10] using leukocyte genomic DNA. Paternally derived clones were predominantly identified for the four DMRs examined (Figure 1a). We next performed combined bisulfite restriction analysis for multiple DMRs, as reported previously.[13] All the autosomal DMRs exhibited markedly skewed methylation patterns consistent with predominance of paternally inherited clones, whereas the *XIST*-DMR on the X chromosome showed a normal methylation pattern (Figure 1a).

Genome-wide microsatellite analysis

Microsatellite analysis was performed for 90 loci with high heterozygosities in the Japanese population.[14] Major peaks consistent with paternal uniparental isodisomy and minor peaks of maternal origin were identified for at least one locus on each chromosome, with the minor peaks of maternal origin being more obvious in tongue and tonsil tissues than in leukocytes (Figure 1b and Supplementary Table 2). There were no loci with three or four peaks indicative of chimerism. The frequency of the androgenetic cells was calculated as 91% in leukocytes, 70% in tongue cells and 79% in tonsil cells, although the estimation apparently was a rough one (for details, see Supplementary Methods).

Expression analysis

We examined *SNRPN* expression, because *SNRPN* showed strong expression in leukocytes (for details, see Supplementary Data). *SNRPN* expression was almost doubled in the leukocytes of this patient (Figure 1c).

DISCUSSION

These results suggest that this patient had an androgenetic 46,XX cell lineage and a normal 46,XX cell lineage. In this regard, both the androgenetic and the biparental cell lineages appear to have derived from a single sperm and a single ovum, because a single haploid genome of paternal origin and that of maternal origin were identified in this patient by genome-wide microsatellite analysis. Thus, it is likely that after a normal fertilization between an ovum and a sperm, the paternally derived pronucleus alone, but not the maternally derived pronucleus, underwent a mitotic division, resulting both in the generation of the androgenetic cell lineage by endoreplication of

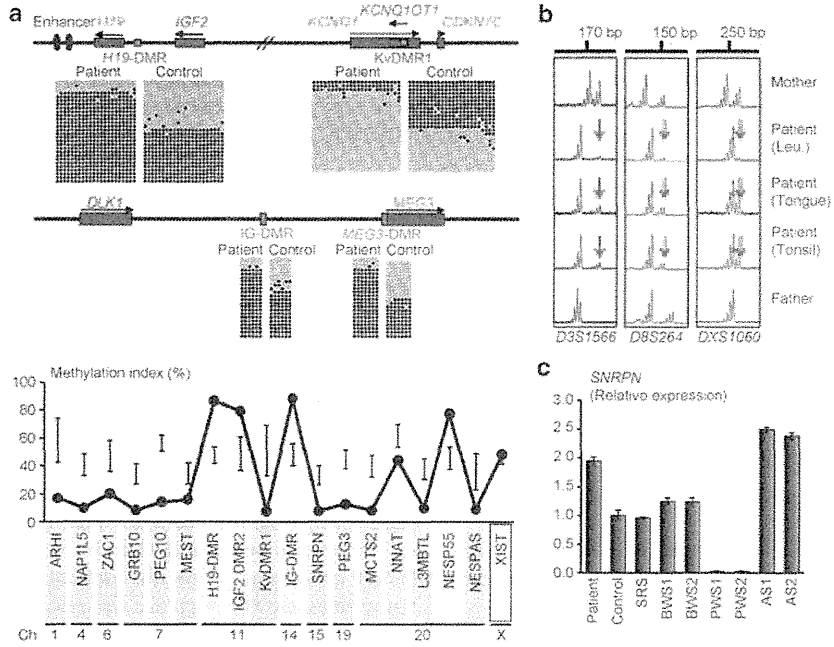

Figure 1 Representative molecular results. (**a**) Methylation analysis. Upper part: Bisulfite sequencing data for the *H19*-DMR and the KvDMR1 on 11p15.5, and those for the IG-DMR and the *MEG3*-DMR on 14q32.2. Each line indicates a single clone, and each circle denotes a CpG dinucleotide; filled and open circles represent methylated and unmethylated cytosines, respectively. Paternally expressed genes are shown in blue, maternally expressed gene in red, and the DMRs in green. The *H19*-DMR, the IG-DMR, and the *MEG3*-DMR are usually methylated after paternal transmission and unmethylated after maternal transmission, whereas the KvDMR1 is usually unmethylated after paternal transmission and methylated after maternal transmission.[10,11] Lower part: Methylation indices (the ratios of methylated clones) obtained from the COBRA analyses for the 18 DMRs. The DMRs highlighted in blue and pink are methylated after paternal and maternal transmissions, respectively. The black vertical bars indicate the reference data (maximum – minimum) in leukocyte genomic DNA of 20 normal control subjects (the *XIST*-DMR data are obtained from 16 control females). (**b**) Representative microsatellite analysis. Major peaks of paternal origin and minor peaks of maternal origin (red arrows) have been identified in this patient. The minor peaks of maternal origin are more obvious in tongue and tonsil tissues than in leukocytes (Leu.). (**c**) Relative expression level (mean ± s.d.) of *SNRPN*. The data are normalized against *TBP*. SRS: an SRS patient with an epimutation (hypomethylation) of the *H19*-DMR; BWS1: a BWS patient with an epimutation (hypermethylation) of the *H19*-DMR; BWS2: a BWS patient with upd(11)pat; PWS1: a Prader-Willi syndrome (PWS) patient with upd(15)mat; PWS2: a PWS patient with an epimutation (hypermethylation) of the *SNRPN*-DMR; AS1: an Angelman syndrome (AS) patient with upd(15)pat; and AS2: an AS patient with an epimutation (hypomethylation) of the *SNRPN*-DMR. The data were obtained using an ABI Prism 7000 Sequence Detection System (Applied Biosystems).

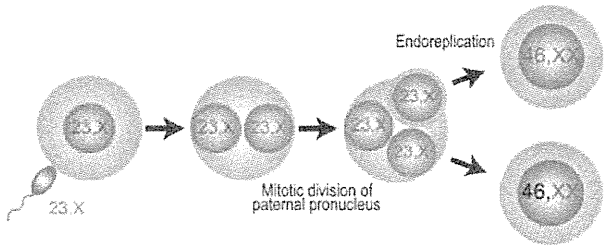

Figure 2 Schematic representation of the generation of the androgenetic/biparental mosaicism. Polar bodies are not shown.

one blastomere containing a paternally derived pronucleus and in the formation of the normal cell lineage by union of paternally and maternally derived pronuclei (Figure 2). This model has been proposed for androgenetic/biparental mosaicism generated after fertilization between a single ovum and a single sperm.[5,15,16] The normal methylation pattern of the *XIST*-DMR is explained by assuming that the two X chromosomes in the androgenetic cell lineage undergo random X-inactivation, as in the normal cell lineage. Furthermore, the results of microsatellite analysis imply that the androgenetic cells were more prevalent in leukocytes than in tongue and tonsil tissues.

A somatic androgenetic cell lineage has been identified in seven liveborn patients including this patient (Supplementary Table 1).[3–7] In this context, leukocytes are preferentially utilized for genetic analyses in human patients, and detailed examinations such as analyses of plural DMRs are necessary to detect an androgenetic cell lineage. Thus, the hitherto identified patients would be limited to those who had androgenetic cells as a predominant cell lineage in leukocytes probably because of a stochastic event and received detailed molecular studies. If so, an androgenetic cell lineage may not be so rare, and could be revealed by detailed analyses as well as examinations of additional tissues in patients with relatively complex phenotypes, as observed in the present patient.

Phenotypic features in androgenetic/biparental mosaicism would be determined by several factors. They include (1) the ratio of two cell lineages in various tissues/organs, (2) the number of imprinted domains relevant to specific features (for example, dysregulation of the imprinted domains on 11p15.5 and 14q32.2 is involved in placentomegaly[9,17]), (3) the degree of clinical effects of dysregulated imprinted domains (an (epi)dominant effect has been assumed for the 11p15.5 imprinted domains[18]), (4) expression levels of imprinted genes in androgenetic cells (although *SNRPN* expression of this patient was consistent with androgenetic cells being predominant in leukocytes, complicated expression patterns have been identified for several imprinted genes in both androgenetic and parthenogenetic fetal mice, probably because of perturbed *cis*- and *trans*-acting regulatory mechanisms[19]) and (5) unmasking of possible paternally inherited recessive mutation(s) in androgenetic cells. Thus, in this patient, it appears that the extent of overall (epi)genetic aberrations exceeded the threshold level for the development of BWS-like and upd(14)pat-like body and placental phenotypes, but remained below the threshold level for the occurrence of other imprinting disorders or recessive Mendelian disorders.

CONFLICT OF INTEREST

The authors declare no conflict of interest.

ACKNOWLEDGEMENTS

This work was supported by grants from the Ministry of Health, Labor, and Welfare, and the Ministry of Education, Science, Sports and Culture.

1 Surani, M. A., Barton, S. C. & Norris, M. L. Development of reconstituted mouse eggs suggests imprinting of the genome during gametogenesis. *Nature* **308,** 548–550 (1984).
2 McGrath, J. & Solter, D. Completion of mouse embryogenesis requires both the maternal and paternal genomes. *Cell* **37,** 179–183 (1984).
3 Hoban, P. R., Heighway, J., White, G. R., Baker, B., Gardner, J., Birch, J. M. *et al.* Genome-wide loss of maternal alleles in a nephrogenic rest and Wilms' tumour from a BWS patient. *Hum. Genet.* **95,** 651–656 (1995).
4 Bryke, C. R., Garber, A. T. & Israel, J. Evolution of a complex phenotype in a unique patient with a paternal uniparental disomy for every chromosome cell line and a normal biparental inheritance cell line. *Am. J. Hum. Genet.* **75**(Suppl), 831 (2004).
5 Giurgea, I., Sanlaville, D., Fournet, J. C., Sempoux, C., Bellanne-Chantelot, C. & Touati, G. Congenital hyperinsulinism and mosaic abnormalities of the ploidy. *J. Med. Genet.* **43,** 248–254 (2006).
6 Wilson, M., Peters, G., Bennetts, B., McGillivray, G., Wu, Z. H., Poon, C. *et al.* The clinical phenotype of mosaicism for genome-wide paternal uniparental disomy: two new reports. *Am. J. Med. Genet. Part A* **146A,** 137–148 (2008).
7 Reed, R. C., Beischel, L., Schoof, J., Johnson, J., Raff, M. L. & Kapur, R. P. Androgenetic/biparental mosaicism in an infant with hepatic mesenchymal hamartoma and placental mesenchymal dysplasia. *Pediatr. Dev. Pathol.* **11,** 377–383 (2008).
8 Jones, K. L. *Smith's Recognizable Patterns of Human Malformation* 6th edn. (Elsevier Saunders: Philadelphia, 2006).
9 Kagami, M., Yamazawa, K., Matsubara, K., Matsuo, N. & Ogata, T. Placentomegaly in paternal uniparental disomy for human chromosome 14. *Placenta* **29,** 760–761 (2008).
10 Kagami, M., Sekita, Y., Nishimura, G., Irie, M., Kato, F., Okada, M. *et al.* Deletions and epimutations affecting the human 14q32.2 imprinted region in individuals with paternal and maternal upd(14)-like phenotypes. *Nat. Genet.* **40,** 237–242 (2008).
11 Yamazawa, K., Kagami, M., Nagai, T., Kondoh, T., Onigata, K., Maeyama, K. *et al.* Molecular and clinical findings and their correlations in Silver-Russell syndrome: implications for a positive role of IGF2 in growth determination and differential imprinting regulation of the IGF2-H19 domain in bodies and placentas. *J. Mol. Med.* **86,** 1171–1181 (2008).
12 Weksberg, R., Shuman, C. & Beckwith, J. B. Beckwith-Wiedemann syndrome. *Eur. J. Hum. Genet.* **18,** 8–14 (2010).
13 Yamazawa, K., Nakabayashi, K., Kagami, M., Sato, T., Saitoh, S., Horikawa, R. *et al.* Parthenogenetic chimaerism/mosaicism with a Silver-Russell syndrome-like phenotype. *J. Med. Genet.* **47,** 782–785 (2010).
14 Ikari, K., Onda, H., Furushima, K., Maeda, S., Harata, S. & Takeda, J. Establishment of an optimized set of 406 microsatellite markers covering the whole genome for the Japanese population. *J. Hum. Genet.* **46,** 207–210 (2001).
15 Kaiser-Rogers, K. A., McFadden, D. E., Livasy, C. A., Dansereau, J., Jiang, R., Knops, J. F. *et al.* Androgenetic/biparental mosaicism causes placental mesenchymal dysplasia. *J. Med. Genet.* **43,** 187–192 (2006).
16 Kotzot, D. Complex and segmental uniparental disomy updated. *J. Med. Genet.* **45,** 545–556 (2008).
17 Monk, D., Arnaud, P., Apostolidou, S., Hills, F. A., Kelsey, G., Stanier, P. *et al.* Limited evolutionary conservation of imprinting in the human placenta. *Proc. Natl. Acad. Sci. USA.* **103,** 6623–6628 (2006).
18 Azzi, S., Rossignol, S., Steunou, V., Sas, T., Thibaud, N., Danton, F. *et al.* Multilocus methylation analysis in a large cohort of 11p15-related foetal growth disorders (Russell Silver and Beckwith Wiedemann syndromes) reveals simultaneous loss of methylation at paternal and maternal imprinted loci. *Hum. Mol. Genet.* **18,** 4724–4733 (2009).
19 Ogawa, H., Wu, Q., Komiyama, J., Obata, Y. & Kono, T. Disruption of parental-specific expression of imprinted genes in uniparental fetuses. *FEBS Lett.* **580,** 5377–5384 (2006).

Supplementary Information accompanies the paper on Journal of Human Genetics website (http://www.nature.com/jhg)